Editors' Suggestion

# Negative tripartite mutual information after quantum quenches in integrable systems

Fabio Caceffo and Vincenzo Alba
*Dipartimento di Fisica dell'Università di Pisa and INFN, Sezione di Pisa, I-56127 Pisa, Italy*

(Received 2 June 2023; accepted 5 October 2023; published 25 October 2023)

We build the quasiparticle picture for the tripartite mutual information (TMI) after quantum quenches in spin chains that can be mapped onto free-fermion theories. A nonzero TMI (equivalently, topological entropy) signals quantum correlations between three regions of a quantum many-body system. The TMI is sensitive to entangled multiplets of more than two quasiparticles, i.e., beyond the entangled-pair paradigm of the standard quasiparticle picture. Surprisingly, for some nontrivially entangled multiplets, the TMI is negative at intermediate times. This means that the mutual information is monogamous, similar to holographic theories. Oppositely, for multiplets that are "classically" entangled, the TMI is positive. Crucially, a negative TMI reflects that the entanglement content of the multiplets is not directly related to the Generalized Gibbs Ensemble (GGE) that describes the postquench steady state. Thus the TMI is the ideal lens to observe the weakening of the relationship between entanglement and thermodynamics. We benchmark our results in the $XX$ chain and in the transverse field Ising chain. In the hydrodynamic limit of long times and large intervals, with their ratio fixed, exact lattice results are in agreement with the quasiparticle picture.

DOI: 10.1103/PhysRevB.108.134434

## I. INTRODUCTION

Recent years witnessed the stunning success of hydrodynamic approaches to describe entanglement dynamics in integrable quantum many-body systems. The so-called quasiparticle picture, which was originally put forward [1] in the context of conformal field theory (CFT), spurred a tremendous amount of activity [2–5]. The tenet of the quasiparticle picture is that in integrable systems after a quantum quench [6–8] the entanglement growth is attributable to the ballistic propagation of entangled *pairs* of quasiparticles. The quasiparticle picture proved to be succesful in generic quenches in free theories [2], as well as in interacting integrable systems [3,9]. Crucially, the quasiparticle picture relies on thermodynamic information. Precisely, in the presence of entangled pairs, the quasiparticles and the entanglement shared between them are extracted from the Generalized Gibbs Ensemble [6] (GGE) that describes the steady state after the quench. The only ingredient of nonthermodynamic origin is the pair structure itself, or, in general, the number of entangled quasiparticles generated after the quench. This entanglement pattern, i.e., the type of entangled multiparticle excitations that are resposible for the entanglement spreading, is enforced by the initial state. Interestingly, the pair structure is related to a special class of "integrable" quenches [10], for which the GGE can be obtained in closed form.

Here we study quantum quenches that give rise to entangled *multiplets* of excitations, through the lens of the tripartite mutual information (TMI). An interesting quench producing entangled multiplets was already explored in Ref. [11]. In that setup, however, the entanglement content of the multiplet is fully determined by the GGE, and it is traced back to a classical-in-nature constraint between the quasiparticles forming the multiplet. Precisely, the focus of Ref. [11] was on quenches in the so-called $XX$ chain (see Sec. II). The prequench initial states were obtained by repeating a unit cell of $n$ sites containing a single fermion. During the postquench dynamics entangled multiplets formed by $n$ quasiparticles are generated. However, as anticipated, the link between entanglement and thermodynamics is only mildly broken because the entanglement between the quasiparticles forming the multiplet can be obtained from the GGE describing the steady state after the quench. We anticipate that this is reflected in the TMI being positive. Interestingly, it was shown in Ref. [12] that it is possible to engineer quantum quenches giving rise to genuinely *quantum-correlated* multiplets. Similar to Ref. [11], entangled multiplets of quasiparticles are produced after the quench. The quasiparticles propagate ballistically, implying that a hydrodynamic description of entanglement spreading is possible. However, the entanglement shared between the quasiparticles cannot be extracted from the GGE. Hence, the link between entanglement dynamics and thermodynamics is strongly broken. As we will show in Sec. VI this leads to negative TMI. Still, even in the presence of multiplets (cf. Refs. [11,12]) standard measures of bipartite entanglement [13–15], such as the von Neumann entropy, exhibit the usual linear growth at short times, followed by a volume-law scaling at asymptotically long times.

Here we show that the tripartite mutual information is a much more revealing tool to highlight the presence of entangled multiplets and the concomitant breaking of the relationship between entanglement and thermodynamics. The TMI became popular [16,17] as a witness of topological order, which is an intrinsically nonlocal quantum correlation. Let us consider a tripartition of a subsystem $A$ as $A = A_1 \cup A_2 \cup A_3$ (see Fig. 1). The tripartite mutual information is defined as [18]

$$I_3 := I_2(A_1 : A_2) + I_2(A_2 : A_3) - I_2(A_2 : A_1 \cup A_3). \quad (1)$$

 

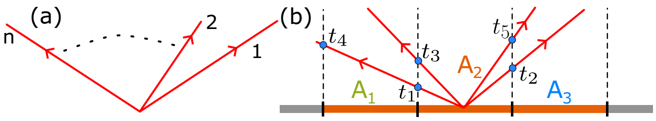


FIG. 1. Multiparticle entangled excitations in spin chains and tripartite mutual information (TMI) dynamics. (a) Example of an entangled multiplet formed by $n$ different quasiparticle species. (b) The TMI [cf. Eq. (1)] measures correlations shared between the three intervals $A_j$ and between them and the rest. Here we focus on three adjacent intervals $A_j$, $j = 1, 2, 3$ of equal length $\ell$. Within the quasiparticle picture, only multiplets that are *shared* between all the intervals $A_j$, and between the intervals and the rest contribute to the TMI. For instance, in (b), we show a quadruplet produced in $A_2$. The circles denote the times at which a quasiparticle changes subsystem. For $t_2 \leqslant t \leqslant t_3$ the quadruplet is shared between all the subsystems, but not with their complement $\bar{A}$. Thus the TMI is zero for $0 \leqslant t \leqslant t_3$. At $t_3$ the leftmost particle leaves $A_1$ and the quadruplet starts to contribute to the TMI.

Here the mutual information $I_2$ measures the correlation between two intervals, and it is defined as

$$I_2(A_i : A_j) := S(A_i) + S(A_j) - S(A_i \cup A_j), \tag{2}$$

where $S(A_j)$ is the von Neumann entropy of subsystem $A_j$. We consider only the case of three adjacent intervals of equal length $\ell$ (see Fig. 1). The generalization to the case of disjoint intervals is straightforward.

The TMI was studied extensively [19] in free quantum field theories (QFTs) (see also Ref. [20] for recent results) at equilibrium. Interestingly, in holographic theories one can show [21] that $I_3 \leqslant 0$, which means that the mutual information is monogamous. This suggests that correlations are genuinely quantum. Indeed, as it is clear from (1), a negative TMI reflects that the correlation shared between the three intervals is more than the sum of the pairwise correlations between them, and hence is quantum-delocalized. Some general results on the sign of the TMI in random states of few qubits was presented in Ref. [22]. It is challenging, however, to obtain the TMI in equilibrium and out-of-equilibrium quantum many-body systems [23–26]. In out-of-equilibrium systems, a negative TMI is routinely used as a fingerprint of the so-called quantum information scrambling [27–29], which is associated with chaotic dynamics. Chaotic systems lack a well-defined notion of quasiparticles, implying that the spreading of quantum information does not happen in a "localized" manner, for instance, via the propagation of entangled quasiparticles. As a result, quantum information is quickly dispersed in the global correlations. A "weak" form of scrambling is present in integrable systems as well [30,31]. A negative TMI was also linked with thermalization in CFTs with a gravity dual [32,33]. The TMI received constant attention in generic CFTs [34–36]. Interestingly, it was shown [37] that in the so-called "minimal-cut" picture for entanglement spreading [38], which is supposed to apply to chaotic systems, the TMI is always negative. This is supported by exact results in random local unitary circuits [39], showing that the TMI decreases linearly with time. Recently, it was shown that [40,41] in one-dimensional models the steady-state TMI after a quantum quench admits a field-theoretical interpretation. Finally, in free-fermion models under continuous monitoring the TMI is negative at any time, and saturates to a negative value in the steady state [42].

Here we show that the TMI can be negative even after quenches in integrable spin chains that can be mapped onto free theories. Precisely, we consider quenches from low-entanglement initial states in the so-called $XX$ chain and in the quantum Ising chain with inhomogeneous transverse field. We focus on quenches that produce entangled multiplets of quasiparticles. For quenches that produce only entangled pairs, the TMI vanishes in the so-called hydrodynamic limit $t, \ell \to \infty$, with fixed ratio $t/\ell$ (see Ref. [43] for a derivation for quenches in the $XY$ chain); this happens because the pairs can entangle only two intervals at a time. For the following, we should stress that all our results hold in the hydrodynamic limit. We show that, despite the presence of multiplets, it is possible to construct a quasiparticle picture for the TMI. First, only multiplets that are shared between the three intervals $A_1$, $A_2$, and $A_3$ and between the intervals and their complement $\bar{A}$ contribute to the TMI [as illustrated in Fig. 1(b)]. This implies that only multiplets formed by $n > 3$ quasiparticles give rise to nonzero TMI, as it was already shown in Ref. [42] in a specific setting. For generic multiplets the TMI can be both positive and negative. For instance, we prove that for the "classical" multiplets considered in Ref. [11] the TMI is positive at all times. Oppositely, for quantum-correlated multiplets (as in Ref. [12]) the TMI attains negative values during the dynamics, although it vanishes at asymptotic long times. Thus a negative TMI is associated with the breaking of the relationship between entanglement and GGE. It is also intriguing to observe that the negative TMI at intermediate times reflects that correlations are nontrivially "scrambled" in the degrees of freedom of the multiplets.

The manuscript is organized as follows. In Sec. II, we introduce the $XX$ chain and the Ising chain with staggered magnetic field. In Sec. III, we discuss the general strategy to construct the quasiparticle picture for the TMI in the presence of generic multiplets. In particular, in Sec. III A, we focus on the states of Ref. [11]. In Sec. III B, we show how the results of Ref. [11] fit into the framework of Sec. III. In Sec. IV, we prove that the "classically" entangled multiplets discussed in Ref. [11] yield positive TMI at all times. In Secs. V and VI, we provide examples of quenches that give negative TMI in the $XX$ chain and in the Ising chain, respectively. In Sec. VII, we benchmark our results against numerical data for the $XX$ chain and the Ising chain (in Secs. VII A and VII B). We present our conclusions in Sec. VIII. In Appendix A we provide an *ab initio* derivation of the quasiparticle picture for the single-interval von Neumann entropy for the same quench discussed in Sec. V.

## II. MODELS AND OUT-OF-EQUILIBRIUM PROTOCOLS

Here we consider the so-called $XX$ chain defined as

$$H = -J \sum_{i=1}^{L} \left(\sigma_i^x \sigma_{j+1}^x + \sigma_j^y \sigma_{j+1}^y\right) + h \sum_{i=1}^{L} \sigma_i^z. \tag{3}$$

Here $\sigma_j^\alpha$, with $\alpha = x, y, z$, are the Pauli matrices. We employ periodic boundary conditions setting $\sigma_{L+1}^\alpha = \sigma_1^\alpha$, and we fix $J = 1$ and $h = 0$.

The $XX$ chain after a Jordan-Wigner transformation is transformed in a tight-binding fermionic chain as

$$H = -\sum_{i=1}^{L}(c_i^\dagger c_{i+1} + c_{i+1}^\dagger c_i), \tag{4}$$

where $c_i^\dagger, c_i$ are standard fermionic operators acting at site $i$ of the chain, and obeying the standard fermionic anticommutation relations $\{c_j, c_l^\dagger\} = \delta_{jl}$. The Hamiltonian can be easily diagonalized through a Fourier transform

$$c_k = \frac{1}{\sqrt{L}}\sum_{j=1}^{L} e^{ikj}c_j, \quad k = \frac{2\pi r}{L}, \ r \in [1, L]. \tag{5}$$

We can rewrite (3) as

$$H = \sum_k \varepsilon(k)c_k^\dagger c_k, \quad \text{with } \varepsilon(k) = -2\cos(k), \tag{6}$$

where $\varepsilon(k)$ gives the single-particle dispersion of the fermions.

We also consider the inhomogeneous transverse field Ising chain, defined as

$$H = J\sum_{i=1}^{L}\sigma_i^x\sigma_{i+1}^x + \sum_{i=1}^{L}h_i\sigma_i^z. \tag{7}$$

Here the magnetic field $h_i$ is site-dependent. In particular, here we consider the case in which $h_j$ has a periodicity $n$, i.e., $h_j = h_{j+n}$. Again, we consider periodic boundary conditions for the spins. The inhomogeneous Ising Hamiltonian (7) after the Jordan-Wigner transformation becomes

$$H = \sum_{j=1}^{L}\left[-\frac{1}{2}(c_j^\dagger c_{j+1}^\dagger + c_j^\dagger c_{j+1} + \text{H.c.}) + h_j c_j^\dagger c_j\right], \tag{8}$$

where $c_j, c_j^\dagger$ are fermionic annihilation and creation operators and again we assume $J = 1$. We should remark that for the Ising chain the Jordan-Wigner transformation introduces some ambiguity in the boundary conditions for the fermions (see Refs. [44,45] for a discussion). For a generic global quantum quench these boundary conditions have no effect on the entanglement dynamics. Here we neglect them, choosing periodic boundary conditions also for the fermions.

For the following, it is crucial to observe that both the tight binding (4) and the fermionic Ising chain (8) can be reduced to the form

$$H = \int_{\mathcal{B}}\frac{dk}{2\pi}\sum_{j=1}^{n}\varepsilon_j(k)\eta_j^\dagger(k)\eta_j(k), \tag{9}$$

The sum over $j$ is a sum over different species of quasiparticles, $\varepsilon_j(k)$ is the dispersion of the individual species, and $\mathcal{B}$ is a reduced Brillouin zone for the different species. In (9), $\eta_j(k)$ is a fermionic operator with quasimomentum $k$ and of species $j$. Crucially, the choice of the different species of quasiparticles depends on the symmetry of the initial state, as we now discuss.

Let us first consider the $XX$ chain, with the prequench initial states $|\Phi^\nu_{\{a_1,\ldots,a_\nu\}}\rangle$ considered in Bertini *et al.* [11]. In the protocol of Ref. [11] the system is prepared in a state obtained from a unit cell of $\nu$ sites repeated $L/\nu$ times. Importantly, in each cell there is a single fermion that can be in a generic pure quantum state. Thus the initial state $|\Phi^\nu_{\{a_1,\ldots,a_\nu\}}\rangle$ is of the form

$$\left|\Phi^\nu_{\{a_1,\ldots,a_\nu\}}\right\rangle = \prod_{j=0}^{L/\nu-1}\left(\sum_{m=1}^{\nu}a_m c_{\nu j+m}^\dagger\right)|0\rangle, \tag{10}$$

where the coefficients $a_m$ are arbitrary, and are normalized as $\sum_{m=1}^{\nu}|a_m|^2 = 1$. The states in (10) are Gaussian, as proved in Ref. [11]. In the following, we refer to states of the form (10) as "classically" entangled states (see Sec. IV).

Let us now observe that states of the form (10) have a nonvanishing overlap (cf. [46]) only with eigenstates of the $XX$ chain of the form [11]

$$\left|\Psi_{k_1,\ldots,k_N}\right\rangle = c_{k_1}^\dagger \ldots c_{k_N}^\dagger|0\rangle, \tag{11}$$

with the conditions

$$N = \frac{L}{\nu}, \quad k_i - k_j \neq 0 \bmod \frac{2\pi}{\nu}, \quad i, j = 1, \ldots, \frac{L}{\nu}. \tag{12}$$

Here the first constraint in (12) takes into account that the number of fermions in the state (10) is $L/\nu$. The second condition ensures that only one quasimomentum (defined modulo $2\pi$) in the set $\mathcal{B}_\nu(k)$,

$$\mathcal{B}_\nu(k) = \left\{k, k + \frac{2\pi}{\nu}, \ldots, k + (\nu-1)\frac{2\pi}{\nu}\right\}, \tag{13}$$

can appear in $|\Psi_{k_1,k_2,\ldots,k_N}\rangle$. Violation of (13) gives zero overlap.

To enforce the constraint (12), we can restrict the Brillouin zone choosing $k \in (\pi - \frac{2\pi}{\nu}, \pi]$. We can define new fermionic operators $\eta_j^\dagger(k)$ as

$$\eta_j^\dagger(k) = c_{k-(j-1)2\pi/\nu}^\dagger, \quad \varepsilon_j(k) = \varepsilon\left(k - (j-1)\frac{2\pi}{\nu}\right), \tag{14}$$

where $\varepsilon(k)$ is the dispersion (6), and $j = 1, \ldots, \nu$ runs over the quasiparticles species. It is clear that by employing (14) the Hamiltonian (6) becomes of the form (9), with $n = \nu$ and the Brillouin zone $\mathcal{B} = (\pi - 2\pi/\nu, \pi]$. Finally, we should remark that although Eq. (9) is only a rewriting of (6), it has the advantage that it is compatible with the translation invariance of the initial state. Moreover, as we will discuss in Sec. III, the correlations, and hence entanglement, generated by the out-of-equilibrium dynamics can be conveniently encoded in the correlation between the species operators $\eta_j$.

For the free fermion chain (4), we also consider the initial state $|\Phi_0\rangle$ defined as

$$|\Phi_0\rangle = \prod_{j=0}^{L/4-1}(c_{4j+1}^\dagger c_{4j+2}^\dagger)|0\rangle. \tag{15}$$

This initial state does not fall into the class of initial states considered in Ref. [11]. Indeed, although the state (15) is constructed from the repetition of a four-site unit cell $|1100\rangle$, the unit cell contains more than one particle. Still, the state (15) is Gaussian, as Wick's theorem applies. The quench from the state (15) was also studied in Ref. [47]. The state has nonzero overlap with the $XX$ chain eigenstates $|\Psi_{k_1,k_2,\dots,k_N}\rangle$ satisfying the constraint that *at most* three quasimomenta (defined modulo $2\pi$) of $\mathcal{B}_4(k)$ (cf. (13)) appear. We anticipate that, in contrast with the states (10), the state (15) gives rise to a negative TMI.

Let us now discuss the case of the inhomogeneous Ising chain. In our out-of-equilibrium protocol, the system is initially prepared in the initial state $|\Psi_0\rangle$, which is the ground state of the Hamiltonian (7) with initial magnetic field $h_j^0 = (h_1^0, h_2^0, \dots, h_n^0)$. The magnetic field is then instantly changed to (cf. (7)) $h_j = (h_1, h_2, \dots, h_n)$ [12].

First, let us diagonalize the postquench Hamiltonian (7) defining the quasiparticle excitations $\eta_j(k)$. Following Ref. [12], we restrict the Brillouin zone to $[0, \pi/n)$. In the limit $L \to \infty$, we can rewrite the Ising Hamiltonian (7) as

$$H = \int_0^{\pi/n} \frac{dk}{2\pi} C^\dagger(k)\mathcal{H}_k C(k), \tag{16}$$

where $C^\dagger$ is the $2n$-dimensional vector of the Fourier transform of the original fermions $c_j$ [cf. Eq. (8)] defined as

$$C^\dagger(k) = (c_k^\dagger, \dots, c_{k+(n-1)\pi/n}^\dagger, c_{-k}, \dots, c_{-k-(n-1)\pi/n}). \tag{17}$$

In (16), $\mathcal{H}_k$ is a $2n \times 2n$ matrix encoding the Hamiltonian (8). To proceed, we can diagonalize $h_k$ by defining new fermions $D_h(k)$ as

$$D_h^\dagger = (d_1^\dagger(k), \dots, d_n^\dagger(k), d_1(-k), \dots, d_n(-k)). \tag{18}$$

The fermions $d(k)$ are defined via the relationship

$$C(k) = U_h(k)D_h(k), \tag{19}$$

with $C(k)$ as in (17). In (19), $U_h$ is a $2n \times 2n$ unitary matrix, which is determined by requiring that in terms of $d_j(k)$ and $d_j(-k)$ the free-fermion Hamiltonian (8) becomes diagonal. For generic $n$, $U_h$ has to be determined numerically. For $n = 1$, one recovers the standard Bogoliubov transformation [44]. Now Eq. (8) becomes

$$H = \int_0^{\pi/n} \frac{dk}{2\pi} \sum_{j=1}^{n} \varepsilon_j^h(k)(d_j^\dagger(k)d_j(k) - d_j(-k)d_j^\dagger(-k)). \tag{20}$$

In (20), $\pm\varepsilon_j^h(k)$, with $\varepsilon_j^h(k) \geqslant 0$ are the eigenvalues of $h_k$ [cf. Eq. (16)] and form the single-particle dispersion. The ground state of (20) is annihilated by all the operators $d(\pm k)$. A similar procedure allows to diagonalize the prequench Hamiltonian, with different sets of operators $D_{h^0}(k)$. The latter are obtained from the original fermions $c_k$ via a different unitary transformations $U_{h^0}(k)$.

Crucially, since the fermionic operators $c_k$ [cf. Eq. (17)] are the same before and after the quench, the operators diagonalizing the pre-quench and postquench Hamiltonians are linked by a unitary transformation as

$$D_h(k) = W(k)D_{h^0}(k), \quad W = U_h^{-1}U_{h^0}. \tag{21}$$

Let us now identify

$$\eta_j(k) = \begin{cases} d_j(k) & j \in [1, n] \\ d_{j-n}^\dagger(-k) & j \in [n+1, 2n] \end{cases}. \tag{22}$$

After employing the definitions in (22) the inhomogeneous Ising chain becomes of the form (9). Again, unlike the homogeneous Ising chain [44,45], for the inhomogeneous one it is not possible in general to obtain analytically the single-particle dispersion $\varepsilon_i(k)$ and the matrices $W(k)$ (21) and $U_h$ (19). However, as they are $2n \times 2n$ matrices, they can be obtained numerically with modest computational cost.

To determine the dynamics of the TMI it is necessary to compute the correlation functions (see Sec. III)

$$\mathcal{C}(k) = \langle 0| \begin{pmatrix} \eta_1 \\ \vdots \\ \eta_{2n} \\ \eta_1^\dagger \\ \vdots \\ \eta_{2n}^\dagger \end{pmatrix} (\eta_1^\dagger \quad \cdots \quad \eta_{2n}^\dagger \quad \eta_1 \quad \cdots \quad \eta_{2n})|0\rangle, \tag{23}$$

where $|0\rangle$ is the ground state of the Ising chain with magnetic field $h^0$, and $\eta_j$ are the operators that diagonalize the Ising chain with magnetic field $h$. It is straightforward to compute the correlator (23) by first using Eq. (21), and then by using that the operators $\eta_j^{(0)}$ of the initial Ising chain annihilate the ground state. Hence we obtain

$$\mathcal{C}(k) = \begin{pmatrix} W(k) & 0 \\ 0 & W^*(k) \end{pmatrix} \mathcal{C}^{(0)} \begin{pmatrix} W^\dagger(k) & 0 \\ 0 & W^T(k) \end{pmatrix}, \tag{24}$$

where $W(k)$ is defined in (21), and $\mathcal{C}^{(0)}$ is a $4n \times 4n$ diagonal matrix $\mathcal{C}_{ij}^{(0)} = \delta_{ij}$ for $i \in [1, n] \cup [3n+1, 4n]$, and zero otherwise. The matrix $\mathcal{C}^{(0)}$ is the correlation of the pre-quench operators $\eta_j^{(0)}$ calculated over the initial state.

## III. QUASIPARTICLE PICTURE IN THE PRESENCE OF ENTANGLED MULTIPLETS

Here we show how to determine the quasiparticle picture for the TMI in the presence of entangled multiparticle excitations. We start from the framework developed in Ref. [12] (see also Ref. [48]).

Let us also assume that the Hamiltonian governing the postquench dynamics can be diagonalized by a set of operators $\eta_1^\dagger(k), \eta_2^\dagger(k), \dots, \eta_n^\dagger(k)$ as in (9). Let us also assume that the two-point correlation function of the fermionic operators $\eta_j(k)$ calculated on the initial state is block-diagonal as

$$\mathcal{C}(k, p) := \langle\Psi_0|\Gamma(k)\Gamma^\dagger(p)|\Psi_0\rangle \propto \delta_{k,p}, \tag{25}$$

where

$$\Gamma^\dagger(k) := (\eta_1^\dagger(k), \dots, \eta_n^\dagger(k), \eta_1(k), \dots, \eta_n(k)). \tag{26}$$

It is straightforward to check that all the protocols we introduced in II satisfy this requirement. We now consider the correlation matrix $\mathcal{C}(k)$ at fixed quasimomentum $k$ but in the space of species. Specifically, we can write

$$\mathcal{C}(k) := \langle\Psi_0|\Gamma(k)\Gamma^\dagger(k)|\Psi_0\rangle = \begin{pmatrix} \mathbb{1} - G^T(k) & F(k) \\ F^\dagger(k) & G(k) \end{pmatrix}, \tag{27}$$

where the correlators $G_{ij}(k)$ and $F_{ij}(k)$ are $n \times n$ matrices defined as

$$G_{ij}(k) := \langle \Psi_0 | \eta_i^\dagger(k) \eta_j(k) | \Psi_0 \rangle, \tag{28}$$

$$F_{ij}(k) := \langle \Psi_0 | \eta_i(k) \eta_j(k) | \Psi_0 \rangle. \tag{29}$$

Notice that since $G_{ij}$ and $F_{ij}$ are not diagonal, they encode nontrivial correlations between the different species of quasiparticles. The von Neumann entropy of a subregion $A$ and generic entanglement-related quantities are obtained from (27) (see Ref. [49]). Indeed, by taking the inverse Fourier transform of $\mathcal{C}(k)$, one obtains the fermionic correlation function $\widetilde{\mathcal{C}}_{nm}$ in real space. From that, the von Neumann entropy is written as [49]

$$S_A = -\mathrm{Tr}\ \widetilde{\mathcal{C}}_A \ln(\widetilde{\mathcal{C}}_A), \tag{30}$$

where $\mathcal{C}_A$ is the correlation matrix restricted to $A$, i.e., with $n, m \in A$.

Before proceeding, let us observe that for any fixed $k$, the correlation matrix $\mathcal{C}(k)$ [cf. Eq. (27)] is the covariance matrix of a Gaussian pure state. This stems from the fact that the $\mathcal{C}$ of the full system can have only the eigenvalues 0,1 because the system is in a pure state and $\mathcal{C}$ has a block structure in quasimomentum space, implying that each block with fixed $k$ can only have eigenvalues 0,1.

The correlation matrix (27) is the main ingredient to build a quasiparticle picture in the presence of entangled multiparticle excitations [12]. In the quasiparticle picture, at time $t = 0$, at each point in space a multiplet is produced, with arbitrary quasimomentum $k$. At later times the quasiparticles forming the multiplet spread, each quasiparticle species propagating with group velocity $v_i(k) = d\varepsilon_i(k)/dk$, with $\varepsilon_i(k)$ the single-particle energies in (9). The growth of the von Neumann entropy of a subsystem $A$ is attributed to the quasiparticles of the same multiplet that are shared between $A$ and the rest.

We now determine the contribution at time $t$ to the entanglement entropy $S_A$ of a region $A$ (see Fig. 1) of an entangled multiplet with quasimomentum $k$. Let us consider the situation in which at time $t$ only a subset $m$ of the $n$ quasiparticles forming the multiplet is in $A$, the remaining ones being in the complement of $A$. The quasiparticles in $A$ correspond to some operators $\eta_{i_1}, \eta_{i_2}, \dots, \eta_{i_m}$, where $1 \leqslant i_p \leqslant n$. We introduce the matrix $\mathcal{C}_A(k, \mathcal{Q}_A)$, with $\mathcal{Q}_A = \{i_p\}_{p=1}^m$ as the correlation matrix $\mathcal{C}(k)$ [cf. Eq. (27)] in which we restrict the row and column indices of $G_{ij}$ and $F_{ij}$ [cf. Eqs. (28) and (29)] to the subset $\mathcal{Q}_A$. Finally, the contribution of this configuration to the entanglement entropy is

$$s(k, \mathcal{Q}_A) = -\mathrm{Tr}\ \mathcal{C}_A \ln(\mathcal{C}_A), \tag{31}$$

where the trace is over the $2m \times 2m$ matrix $\mathcal{C}_A(k)$. Again, in (31) $\mathcal{Q}_A$ are the indices of the quasiparticles that are in $A$. Notice that $s(k, \mathcal{Q}_A) = s(k, \mathcal{Q}_{\bar{A}})$. This is due to the fact that $\mathcal{C}(k)$ defines a Gaussian pure state. Finally, the entanglement entropy $S_A$ is obtained as

$$S_A = \int_{\mathcal{B}} \frac{dk}{2\pi} \sum_{\mathcal{Q}_A} \mathcal{D}(k, \mathcal{Q}_A, \ell, t) s(k, \mathcal{Q}_A). \tag{32}$$

Here the sum is over all the possible ways of distributing the quasiparticles forming the entangled multiplet between $A$ and its complement. In (32), $\mathcal{D}(k, \mathcal{Q}_A, \ell, t)$ is a kinematic factor that counts the number of entangled multiplets with fixed $k$ created at $t = 0$ and that at time $t$ give rise to the configuration $\mathcal{Q}_A$. The factor $\mathcal{D}(k, \mathcal{Q}_A, \ell, t)$ depends on time and on the length $\ell$ of $A$. Moreover, it depends on $k$ through the velocities $\varepsilon'_j(k)$ of the quasiparticles.

Finally, we should stress that although the presence of entangled multiplets does not invalidate the quasiparticle picture for entanglement spreading, the entanglement content $s(k, \mathcal{Q}_A)$ of the quasiparticles is not directly related to the thermodynamic entropy of the GGE that describes the steady state, unlike the case in which only entangled pairs of quasiparticles are produced after the quench [1–3]. In particular, the entanglement content does not depend only on the diagonal correlations in (28) that represent the root densities of the excitations

$$\rho_j(k) := \langle \Psi_0 | \eta_j^\dagger(k) \eta_j(k) | \Psi_0 \rangle, \tag{33}$$

while the GGE contains information only about these densities [12]. Let us briefly discuss the relationship between entanglement entropy and GGE thermodynamic entropy in quenches in free-fermion systems [9]. First, in the limit $t \to \infty$ after a quench from typical initial states, it is well established that local observables reach a stationary value, which is describable via a statistical ensemble. Since free-fermion models are integrable, this is not the usual Gibbs ensemble [7]. The correct ensemble is the so-called Generalized Gibbs Ensemble (GGE), which can be fully determined by the occupations $\rho_j(k)$ in (33). Importantly, in the thermodynamic limit $L \to \infty$ there is an exponentially diverging number of *microscopic* eigenstates of the model that give rise to the same GGE, or, equivalently, to the same occupations $\rho_j(k)$. In the thermodynamic limit, expectation values of local observables over these eigenstates become the same. The logarithm of the number of microscopic eigenstates that give rise to the same thermodynamic *macrostate* is given by the so-called Yang-Yang entropy [5] $S_{YY}$ defined as

$$S_{YY} := L \sum_j \int_{-\pi}^{\pi} \frac{dk}{2\pi} s_j^{YY}(j, k), \tag{34}$$

where [5]

$$s_j^{YY} = \rho_j(k) \ln(\rho_j(k)) + (1 - \rho_j(k)) \ln(1 - \rho_j(k)). \tag{35}$$

Nevertheless, in all the cases we take into account, the relationship between the entanglement content and the thermodynamic entropy of the GGE is recovered in the limit $t/\ell \to \infty$, because in this limit the particles of a multiplet are too far from each other, and only one of them is in $A$. Having $F_{ij} = 0$ in all the cases that we consider, (see below), the von Neumann entropy density $S_A/\ell$ depends only on the root densities (33) and, precisely, reduces to the thermodynamic entropy density $S_{YY}/L$ [cf. Eq. (34)] of the GGE.

To conclude, let us illustrate the formalism for the case of the quench from the Néel state. The Néel state $|101010\cdots\rangle$ corresponds to $n = \nu = 2$ in (10) and to $a_1 = 1$ and $a_2 = 0$. Now, we have $\eta_1^\dagger = c_k^\dagger$ [cf. Eqs. (9) and (14)] and $\eta_2^\dagger = c_{k-\pi}^\dagger$, with $k \in (0, \pi]$. The pairing terms $F_{ij}$ [cf. Eq. (29)] are identically zero for the Néel quench. Moreover, $G_{jl} = 1/2\ \delta_{jl}$ [cf. Eq. (28)] is diagonal and independent of $k$. Now, it is clear that there are only two ways of distributing the members of the pair between $A$ and the complement. Precisely, one has $\mathcal{Q}_A(k) = \{1\}$ or $\mathcal{Q}_A(k) = \{2\}$ [cf. Eq. (32)]. Notice that the energy of the two species of quasiparticles is $\varepsilon_1(k) = \varepsilon(k)$ and $\varepsilon_2(k) = \varepsilon(k - \pi)$, with $\varepsilon$ defined in (6). This implies that $v_1 = \varepsilon_1'(k) = -v_2$. The kinematic function $\mathcal{D}(k, \mathcal{Q}_A, \ell, t)$ [cf. Eq. (32)] counts the number of pairs that are in the configuration $\mathcal{Q}_A$ at time $t$. It is clear that for $\mathcal{Q}_A = \{1\}$, one has that $\mathcal{D}(k, \{1\}, \ell, t)$ takes contribution from the pairs created on the region near the left edge, which gives a contribution $\min(2v_1(k)t, \ell)$. The contribution of species 2 is the same. Finally, it is clear that $s(k, \{1\}) = s(k, \{2\}) = \ln(2)$. This implies that

$$S_A = 2 \int_0^{\pi} \frac{dk}{2\pi} \min(2v_1(k)t, \ell) \ln(2), \tag{36}$$

which is the well-known quasiparticle picture for the von Neumann entropy after the quench from the Néel state in the $XX$ chain [9].

### A. An example of "classically" entangled multiplets: the states of Bertini *et al.*

In the last section, we showed that the presence of nontrivially entangled multiplets of excitations implies that the dynamics of the von Neumann entropy cannot be always described in terms of the densities of excitations $\rho_j(k)$ [cf. Eq. (33)]. Still, as it has been pointed out in Ref. [11] (see also Ref. [12]) the out-of-equilibrium dynamics starting from the states $|\Phi^{\nu}_{\{a_1,\dots,a_\nu\}}\rangle$ [cf. Eq. (10)] in the $XX$ chain gives rise to "classically" entangled multiplets. As we will show in Sec. IV, this implies that the TMI is positive at all times.

Let us now review the quasiparticle picture for the von Neumann entropy for quenches starting from the states $|\Phi^{\nu}_{a_1,a_2,\dots,a_\nu}\rangle$ [cf. Eq. (10)]. Crucially, for this class of states the contribution of the entangled multiplets to the entropies is obtained in terms of the densities of the quasiparticles $\rho_j(k)$, which are defined as

$$\rho_j(k) = \langle \Phi^{\nu} | \eta_j^{\dagger}(k) \eta_j(k) | \Phi^{\nu} \rangle, \tag{37}$$

where $\eta_j(k)$ are defined in (14). A structure similar to the one outlined in III emerges.

The initial state acts as a source of entangled multiplets of one particle and $\nu - 1$ holes. However, in contrast with the general picture of Sec. III, the contribution of these multiplets is entirely written in terms of $\rho_j(k)$. Again, at a generic time $t$ we can consider the situation in which only a subset of the quasiparticles forming the multiplet is in $A$. Let us consider the case with $m$ quasiparticles $\eta_j$ with $j \in \mathcal{Q}_A$ in $A$. Let us define $\rho_{\text{in}}(k)$ as

$$\rho_{\text{in}}(k) = \sum_{j \in \mathcal{Q}_A} \rho_j(k). \tag{38}$$

The contribution of this configuration to the entanglement between $A$ and the rest is [11]

$$s(k, \mathcal{Q}_A) = -\rho_{\text{in}} \ln(\rho_{\text{in}}) - (1 - \rho_{\text{in}}) \ln(1 - \rho_{\text{in}}). \tag{39}$$

Notice that since the state of the system is pure, if all the quasiparticles are in $A$ one has $s(k, \mathcal{Q}_A) = 0$. This means that $\sum_j \rho_j = 1$. This constraint automatically implies that $s(k, \mathcal{Q})_A = s(k, \mathcal{Q}_{\bar{A}})$.

From (39), we obtain the entropy $S_A$ as

$$S_A = \int_{\pi(1-2/\nu)}^{\pi} \frac{dk}{2\pi} \sum_{\mathcal{Q}_A} \mathcal{D}(k, \mathcal{Q}_A, \ell, t) s(k, \mathcal{Q}_A). \tag{40}$$

Here $s(k, \mathcal{Q}_A)$ is the entanglement content due to the configuration with the quasiparticles in $\mathcal{Q}_A$ being in $A$ and it is given in (39). In (40), the kinematic term $\mathcal{D}(k, \mathcal{Q}_A, \ell, t)$ counts the number of multiplets with fixed $k$ that are in $\mathcal{Q}_A$.

### B. Equivalence with the general method

Let us show that the approach of Ref. [11] outlined in Sec. III A corresponds to a particular case of the framework introduced in Sec. III. We first observe that for the states $|\Phi^{\nu}_{\{a_1,\dots,a_\nu\}}\rangle$ one has that $F_{ij} = 0$ [cf. Eq. (29)]. Moreover, we have that

$$\langle \Phi^{\nu} | c_k^{\dagger} c_{k'} | \Phi^{\nu} \rangle \neq 0 \quad \text{only if } \nu(k - k') = 0\,[\text{mod}\, 2\pi], \tag{41}$$

which follows from the $\nu$-site translation invariance. Now, Eq. (27) is block diagonal as

$$\mathcal{C}(k) = \begin{pmatrix} \mathbb{1} - G^T(k) & 0 \\ 0 & G(k) \end{pmatrix}. \tag{42}$$

Following the strategy of Sec. III, we have to determine the entanglement entropy associated to a partition $\mathcal{Q}_A$ of the $\nu$ quasiparticles forming the entanglement multiplet. This is given by (31). It is straightforward to show that (31) becomes the same as (40) provided that $G$ [cf. Eq. (42)] has rank one. Indeed, if the rank of $G$ is one, any submatrix $G_A(k)$ will have rank at most one. This means that its nonzero eigenvalue is $\text{Tr}(G_A(k))$, with

$$\text{Tr}(G_A) = \sum_{j \in \mathcal{Q}_A} \langle \Phi^{\nu} | \eta_j^{\dagger} \eta_j | \Phi^{\nu} \rangle = \rho_{\text{in}}(k), \tag{43}$$

where $\rho_{\text{in}}$ is defined in (38). Finally, for a given set $\mathcal{Q}_A$ of quasiparticles in $A$, one obtains that the contribution $s(k, \mathcal{Q}_A)$ to the von Neumann entropy is $s(k, \mathcal{Q}_A) = -\text{Tr}\, \mathcal{C}_A \ln(\mathcal{C}_A)$ (cf. (42)), and by using (43), it coincides with (39).

To conclude, we have to show that $G(k)$ for the generic state $|\Phi^{\nu}\rangle$ has rank one. By using the definition of $\eta_j(k)$ [cf. Eq. (14)], we obtain

$$\begin{aligned} G_{jl}(k) &= \langle \Phi^{\nu} | \eta_j^{\dagger}(k) \eta_l(k) | \Phi^{\nu} \rangle \\ &= \frac{1}{L} \sum_{m,n=1}^{L} e^{-i(k-(j-1)2\pi/\nu)m + i(k-(l-1)2\pi/\nu)n} \langle c_m^{\dagger} c_n \rangle \\ &= \frac{1}{\nu} \sum_{m,n=1}^{\nu} e^{-i(k-(j-1)2\pi/\nu)m} e^{i(k-(l-1)2\pi/\nu)n} \langle c_m^{\dagger} c_n \rangle \\ &= \frac{1}{\nu} \sum_{m,n=1}^{\nu} e^{-i(k-(j-1)2\pi/\nu)m} a_m^* e^{i(k-(l-1)2\pi/\nu)n} a_n, \end{aligned} \tag{44}$$

where we defined $\langle c_m^{\dagger} c_n \rangle := \langle \Phi^{\nu} | c_m^{\dagger} c_n | \Phi^{\nu} \rangle$. In the second row in (44) we exploited translation invariance. The coefficients $a_j$ are defined in (10). Now, it is clear that $G_{jl}$ has rank one for any $a_j$ because it is an outer product of two vectors.

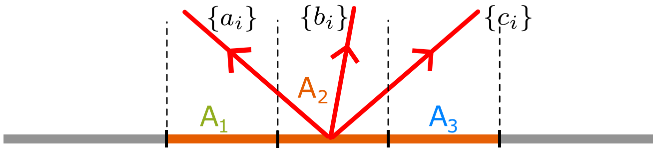


FIG. 2. A typical entangled multiplet contributing to the dynamics of the tripartite mutual information (TMI). The entangled multiplet is created at $t = 0$ in subsystem $A_2$, and it consists of $n$ quasiparticles with labels $\mathcal{Q} = \{1, 2, \dots, n\}$. Here we denote as $\{a_i\} \subseteq \mathcal{Q}$ the quasiparticles in $A_1$. Similarly, we define $\{b_i\}$ and $\{c_i\}$ as the quasiparticles in $A_2$ and $A_3$, respectively. The entanglement entropy of the interval $A_1$ is obtained from the restricted correlation matrix $\mathcal{C}_{A_1}(k)$ [cf. Eq. (27)] whose $F$ and $G$ blocks have row and column indices in $\{a_i\}$.

## IV. CLASSICALLY ENTANGLED MULTIPLETS YIELD NON-NEGATIVE TMI

We now show that for all the quenches from the "classically" entangled states (10), the tripartite mutual information (TMI) between three generic intervals is always non-negative in the hydrodynamic limit. Here for the sake of simplicity we consider the case of three equal adjacent intervals of length $\ell$ (see Fig. 2). The hydrodynamic limit is defined as $\ell, t \to \infty$ with their ratio $t/\ell$ fixed.

Given a generic entangled multiplet formed by $n$ quasiparticles, to build the quasiparticle picture for the TMI, we have to first identify the different ways of distributing the quasiparticles among the three subsystems. Let us denote by $\{a_i\}$, with $1 \leqslant a_i \leqslant n$ the set of indices identifying the quasiparticles that at a generic time $t$ after the quench are within $A_1$. Similarly, we can introduce $\{b_i\}$ and $\{c_i\}$ as the indices of the quasiparticles in $A_2$ and $A_3$, respectively (see Fig. 2). Notice that in general $\{a_i\} \cup \{b_i\} \cup \{c_i\}$ is not the full multiplet. Indeed, as it will be clear in the following, for the configuration to contribute to the TMI the multiplet has to be shared also with the complement of $A = A_1 \cup A_2 \cup A_3$.

We can define the contribution $\tau_3$ of the quasiparticles to $I_3$ as

$$\begin{aligned}\tau_3(k, \{a_i\}, \{b_i\}, \{c_i\}) &= s_{\{a_i\}\cup\{b_i\}\cup\{c_i\}}(k) - s_{\{a_i\}\cup\{b_i\}}(k) - s_{\{a_i\}\cup\{c_i\}}(k)\\ &\quad - s_{\{b_i\}\cup\{c_i\}}(k) + s_{\{a_i\}}(k) + s_{\{b_i\}}(k) + s_{\{c_i\}}(k). \end{aligned}\tag{45}$$

Precisely, the TMI is given as

$$I_3(t) = \sum_{\{a_i\},\{b_i\},\{c_i\}} \int_{\pi-\frac{2\pi}{\nu}}^{\pi} \frac{dk}{2\pi} \tau_3(k)\mathcal{D}(k, \ell, t), \tag{46}$$

where the sum is over the ways of distributing the quasiparticles forming the mutliplet among the three subsystems, and $\mathcal{D}(k, \ell, t)$ is a kinematic factor that describes the propagation of the quasiparticles forming the multiplet. For the von Neumann entropy and for the quenches that produce entangled pairs one has that $\mathcal{D}(k, \ell, t) = \min(2v(k)t, \ell)$. In Eq. (45), $s_X$ is the contribution to the von Neumann entropy due to the quasiparticles $X$ being within the subsystem, and the remaining ones outside of it. In (45), $s_X$ is obtained as the entropy of the reduced correlation matrix $\mathcal{C}_X(k)$ [cf. Eq. (31)]. $\mathcal{C}_X$ is obtained from $\mathcal{C}(k)$ [cf. Eq. (27)] by selecting the rows and columns in $X$. In (45), the first contribution is associated with the last term in (1), i.e., with the entropy of $A_1 \cup A_2 \cup A_3$.

Let us now discuss some constraints on $\{a_i, b_i, c_i\}$ to ensure a nonzero contribution to $\tau_3$. First, configurations without at least a quasiparticle in each of the three intervals $A_1$, $A_2$, and $A_3$ give $\tau_3 = 0$. Indeed, without loss of generality we can assume that $\{a_i\} = \emptyset$, i.e., there are no quasiparticles in $A_1$ (see Fig. 2). Then, from (45), and using that $s_\emptyset(k) = 0$, we have $\tau_3 = 0$.

An important consequence is that one has nonzero $\tau_3$ only for $n \geqslant 3$, i.e., when triplets or larger multiplets are produced after the quench. However, as shown in Ref. [42], even for $n = 3$, i.e., for entangled triplets, the tripartite information is zero. Let us briefly recall the proof of this result. The only quasiparticle configuration that has to be considered is that with a quasiparticle in each interval $A_j$. Without loss of generality, we can assume $\{a_i\} = \{1\}$, $\{b_i\} = \{2\}$, $\{c_i\} = \{3\}$ because the result does not depend on the permutation of the labels of the quasiparticles. Now, since for any system in a pure state we have that $S_A = S_{\bar{A}}$, we obtain that (see Sec. III) $s_{\{1,2,3\}} = s_\emptyset = 0$, $s_{\{1,2\}} = s_{\{3\}}$, $s_{\{2,3\}} = s_{\{1\}}$ and $s_{\{1,3\}} = s_{\{2\}}$. It is straightforward to check that this implies that $\tau_3(k) = 0$ [cf. Eq. (45)].

Thus the simplest case in which there can be nonzero tripartite information is that of the entangled *quadruplets* ($n = 4$). Again, the entanglement content remains the same under exchange of the quasiparticles inside and outside of the subsystem of interest. This implies that if all the four quasiparticles are in $A = A_1 \cup A_2 \cup A_3$, $\tau_3$ vanishes. Clearly, the only nontrivial configuration that contributes to $\tau_3$ is that with one quasiparticle in each interval $A_1$, $A_2$, and $A_3$, and one quasiparticle outside of $A$. In the following, we are going to show that for the "classically" entangled states introduced in Sec. IV, one has $\tau_3 > 0$ for any $k$, which implies that the tripartite information is positive at any time. Specifically, for $n = 4$, Eq. (45) (see Fig. 2) becomes

$$\begin{aligned}\tau_3(k) &= s_{\{1,2,3\}}(k) - s_{\{1,2\}}(k) - s_{\{2,3\}}(k) - s_{\{1,3\}}(k)\\ &\quad + s_{\{1\}}(k) + s_{\{2\}}(k) + s_{\{3\}}(k). \end{aligned}\tag{47}$$

Following [11], Eq. (47) can be rewritten [cf. Eq. (38) and (39)] as

$$\begin{aligned}\tau_3(k) &= f(a+b+c) - f(a+b) - f(a+c) - f(b+c)\\ &\quad + f(a) + f(b) + f(c), \end{aligned}\tag{48}$$

where [cf. Eq. (39)]

$$f(x) = -x\ln(x) - (1-x)\ln(1-x), \tag{49}$$

with

$$a = \rho_1(k), \quad b = \rho_2(k), \quad c = \rho_3(k). \tag{50}$$

The total density is constrained as $\sum_{j=1}^n \rho_j(k) = 1$, and the variables $a, b, c$ satisfy $a \geqslant 0$, $b \geqslant 0$, $c \geqslant 0$ and $a + b + c \leqslant 1$. The expression in (48) is always non-negative under the given constraints on the densities $a$, $b$ and $c$. Indeed, one can easily check that $\tau_3$ [cf. Eq. (48)] is smooth as a function of $a, b, c$, and it vanishes at the boundaries of the allowed region for $a, b, c$. Moreover, Eq. (48) has a unique stationary point at $a = b = c = 1/4$, where it is positive. This allows us to conclude that $\tau_3 > 0$ for any $a, b, c$, except at the boundaries where $\tau_3 = 0$. Notice that the boundaries ($a = 0$, $b = 0$, $c = 0$) correspond to the cases with at least one of the intervals $A_1$, $A_2$, and $A_3$ not containing a quasiparticle, that do not contribute to the TMI.

Let us now consider the general case with arbitrary $n$-plets with $n > 4$. Specifically, let us consider the situation in which quasiparticles with indices $\{a_j\}_{j=1}^p$ are in $A_1$, those with $\{b_j\}_{j=1}^q$ in $A_2$, and with $\{c_j\}_{j=1}^r$ in $A_3$. We have $p + q + r \leqslant n$. Crucially, Eq. (45) has the same form as (48) with different $a$, $b$ and $c$, that are defined as

$$a = \sum_{j=1}^{p} \rho_{a_j}(k), \quad b = \sum_{j=1}^{p} \rho_{b_j}(k), \quad c = \sum_{j=1}^{r} \rho_{c_j}(k). \tag{51}$$

Moreover, the $a$, $b$, $c$ in (51) satisfy the same constraint, i.e., $a \geqslant 0$, $b \geqslant 0$, $c \geqslant 0$, $a + b + c \leqslant 1$, as in the case of quadruplets [cf. Eq. (50)]. This implies that $\tau_3(k) \geqslant 0$ for any $k$, which allows us to conclude that the TMI cannot be negative for the "classically" entangled states of Ref. [11].

## V. NEGATIVE TMI AFTER A QUENCH IN THE *XX* CHAIN

Having established in the previous section that quenches starting from states of the form (10) in the free fermion chain studied in Ref. [11] give rise to a non-negative tripartite mutual information, we now provide a setup in which $I_3(t)$ is *negative* at intermediate times in the hydrodynamic limit.

Precisely, let us now consider the quench in the $XX$ chain starting from the state $|\Phi_0\rangle$ [cf. Eq. (15)]. The state exhibits a four-site translation invariance. The dynamics from $|\Phi_0\rangle$ produces entangled quadruplets, and in contrast with the states considered in Ref. [11], contains two fermions per unit cell. This implies that the correlation matrix $G_{ij}(k)$ [cf. Eq. (28)] has rank larger than one [the last step in (44) does not hold]. Crucially, this means that the von Neumann entropy is not straightforwardly obtained from the fermionic occupations $\rho_j(k)$ [cf. Eq. (33)], i.e., from the GGE that describes the steady state.

Before proceeding, let us observe that since the initial state has a well defined fermion number, one has that $F_{ij}(k) = 0$ [cf. Eq. (29)] at any time after the quench. Now, we restrict the Brillouin zone to $\mathcal{B} = (\pi/2, \pi]$, and define the four quasiparticles $\eta_j(k)$, $j \in [1, 4]$ according to (14). The associated group velocities are

$$v_j(k) = \frac{d}{dk}\varepsilon_j(k) = 2\sin\left(k - (j-1)\frac{\pi}{2}\right), \tag{52}$$

where $\epsilon_j(k)$ are the dispersions of the different species [cf. Eq. (14)]. As it is clear from (52), $v_1$ and $v_2$ are positive in the reduced Brillouin zone, while $v_3 = -v_1$ and $v_4 = -v_2$.

Furthermore, a straightforward calculation gives the fermionic correlation matrix $G(k)$ [cf. Eq. (28)] as

$$G(k) = \frac{1}{4}\begin{pmatrix} 2 & -1-i & 0 & -1+i \\ -1+i & 2 & -1-i & 0 \\ 0 & -1+i & 2 & -1-i \\ -1-i & 0 & -1+i & 2 \end{pmatrix}. \tag{53}$$

Notice that $G(k)$ does not depend on $k$, similarly to the quench from the fermionic Néel state [46].

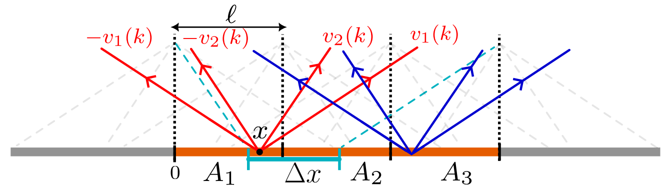


FIG. 3. A typical entangled multiplet with $\nu = 4$ contributing to the dynamics of the tripartite mutual information TMI in the $XX$ chain after the quench from the state $|\Phi_0\rangle = |\uparrow\uparrow\downarrow\downarrow\rangle^{\otimes L/4}$. We consider the TMI $I_3$ between three equal intervals $A_i$ of length $\ell$. We show the contribution of an entangled quadruplet produced at a generic position $x$. Here we consider the case with the group velocities of the quasiparticles being $v_1(k)$, $v_2(k) \geqslant 0$, $v_3(k) = -v_1(k)$, and $v_4(k) = -v_2(k)$. The different colors show the two types of quadruplets that contribute to $I_3$. They correspond to the situation in which $A$ is entangled with $\bar{A}$ via the left and right boundary, respectively. For the first case, the total number of multiplets contributing to $I_3$ is proportional to the width $\Delta x$.

We are now ready to discuss the quasiparticle picture for the dynamics of the TMI. The direct calculation of the tripartite information within the quasiparticle picture is somewhat easier than the calculation of the entropies. Specifically, the reason is that the only quasiparticle configurations yielding nonzero TMI are those with exactly one particle inside each of the three intervals and one outside of $A$. From the velocities (52) it is straightforward to realize that there are only four ways to satisfy this condition, which depend on the ordering of the velocities. Specifically, we have to consider the two cases.

(i) For $\pi/2 \leqslant k \leqslant 3/4\pi$, one has $v_1(k) \geqslant v_2(k) \geqslant 0$ and $v_3(k) \leqslant v_4(k) \leqslant 0$. Now, there are only two possibilities to have nonzero $I_3$. The first one is that the quasiparticle of species 1 is in $A_3$, that of species 2 is in $A_2$, and that of species 4 in $A_1$, with the quasiparticle of species 3 outside of $A$ on the left. The other possibility is that the quasiparticle of species 1 is outside of $A$ on the right, that of species 2 is in $A_3$, that of species 4 in $A_2$, and that of species 3 is in $A_3$. These two configurations are depicted in Fig. 3 with different colors.

(ii) For $3/4\pi \leqslant k \leqslant \pi$, one has $v_2(k) \geqslant v_1(k) > 0$ and $v_4(k) \leqslant v_3(k) \leqslant 0$. The configurations that contribute to the TMI are the same as in (*i*) after the exchanges $1 \leftrightarrow 2$ and $3 \leftrightarrow 4$.

It is straightforward to obtain the total number of configurations contributing to $I_3$. Let us focus on the first type (i). Let us consider an entangled multiplet produced at a generic point $x$ at $t = 0$. We only consider the situation in which the leftmost quasiparticle is outside of $A$ on the left (see Fig. 3). The conditions that give nonzero $I_3$ are

$$x \geqslant v_2 t, \quad x \geqslant \ell - v_2 t, \quad x \geqslant 2\ell - v_1 t, \tag{54}$$

together with

$$x \leqslant v_1 t, \quad x \leqslant \ell + v_2 t, \quad x \leqslant 2\ell - v_2 t, \quad x \leqslant 3\ell - v_1 t. \tag{55}$$

As it is clear from Fig. 3, the constraints above identify the region of width $\Delta x$ in which the quadruplets that contribute to $I_3$ are produced at $t = 0$. After integrating over all the possible positions $x$, one obtains

$$\mathcal{D}_1(k,\ell,t) = \max\{\min\{v_1t, \ell+v_2t, 2\ell-v_2t, 3\ell-v_1t\} - \max\{v_2t, \ell-v_2t, 2\ell-v_1t\}, 0\}. \quad (56)$$

The entangled quadruplets of type $(i)$ in which the rightmost particle is outside of $A$ give

$$\mathcal{D}_2(k,\ell,t) = \max\{\min\{\ell+v_1t, 2\ell+v_2t, 3\ell-v_2t\} - \max\{v_1t, \ell+v_2t, 2\ell-v_2t, 3\ell-v_1t\}, 0\}. \quad (57)$$

Together with (56) and (57), there are two contributions $\mathcal{D}_3$ and $\mathcal{D}_4$, which are obtained by exchanging $v_1 \leftrightarrow v_2$ and $v_3 \leftrightarrow v_4$.

To proceed, we now determine the contribution of the entangled multiplets to the TMI. This is straightforward using the strategy discussed in Sec. III. Specifically, by using (31) and (53) one can verify that the contribution $\tau_3(k)$ [cf. Eq. (45)] does not depend on $k$ and on the different ways $\mathcal{Q}_A$ of distributing the quasiparticles in the subsystems. We obtain $\tau_3$ as

$$\tau_3 = 2f\left(\frac{1}{2}\right) - 4f\left(\frac{2+\sqrt{2}}{4}\right) < 0, \quad (58)$$

where $f(x)$ is given in (49). Crucially, $\tau_3$ is negative for any $k$. Putting together (56), (57) and (58), we obtain

$$I_3(t) = \left[2f\left(\frac{1}{2}\right) - 4f\left(\frac{2+\sqrt{2}}{4}\right)\right] \times \left(\int_{\pi/2}^{3\pi/4} \frac{dk}{2\pi}[\mathcal{D}_1(k,\ell,t)+\mathcal{D}_2(k,\ell,t)] + \int_{3\pi/4}^{\pi} \frac{dk}{2\pi}[\mathcal{D}_3(k,t,\ell)+\mathcal{D}_4(k,t,\ell)]\right). \quad (59)$$

Finally, the two terms in (59) give the same result. Thus we can rewrite (59) as

$$I_3(t) = \left[4f\left(\frac{1}{2}\right) - 8f\left(\frac{2+\sqrt{2}}{4}\right)\right] \times \int_{\pi/2}^{3\pi/4} \frac{dk}{2\pi}[\mathcal{D}_1(k,\ell,t)+\mathcal{D}_2(k,\ell,t)]. \quad (60)$$

We should mention that the terms in $\tau_3(k)$ in (58) appear naturally in the quasiparticle picture for the von Neumann entropy of a single interval (see Appendix A for an *ab initio* derivation). Let us discuss the dynamics of $I_3$ as obtained from (60). In the following, we refer to times such that $t, \ell \to \infty$ with $t/\ell \ll 1$ as short times, whereas by asymptotically long times we mean the situation with $t, \ell \to \infty$ with $t/\ell \to \infty$. At short times, $I_3 = 0$, and it remains zero up to time $t = \ell/(\max(v_1(k), v_2(k)))$, when the quasiparticles forming the quadruplets start being shared between all the subsystems. At later times, $I_3$ decreases, reaching a minimum. Finally, it vanishes at asymptotically long times, when the particles of each multiplet are too far from each other to be shared between all the subsystems. It is interesting to investigate the behavior of the integrand in (60) as a function of time. As it is clear from the derivation of (56) and (57), the integrand is the width

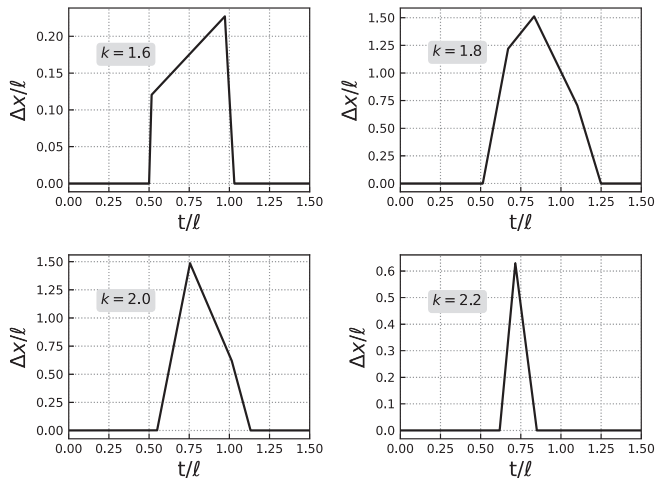


FIG. 4. Tripartite mutual information (TMI) in the $XX$ chain after the quench from the state $|\Phi_0\rangle$ [cf. Eq. (15)]. We show $\Delta x/\ell$, with $\Delta x = \mathcal{D}_1 + \mathcal{D}_2$ [cf. Eq. (60)]. We plot $\Delta x/\ell$ for fixed quasimomentum $k$ versus $t/\ell$. Notice that apart for a constant, $\Delta x$ is the contribution of the quasiparticles to $I_3$. The different panels correspond to different $k$. The cusplike features are due to the presence of quasiparticles with different velocities.

of the spatial region where the entangled multiplets that at a given time give nonzero $I_3$ are produced. In Fig. 4, we report $\Delta x/\ell$, with $\Delta x = \mathcal{D}_1 + \mathcal{D}_2$. As anticipated, $I_3$ is zero at short times. This corresponds to the fact that at short times there are no entangled quadruplets that are shared among the three subsystems $A_j$ and the rest. Moreover, one should observe that at intermediate times the behavior of $I_3$ is quite involved and it depends dramatically on the quasimomentum $k$. Specifically, $\Delta x/\ell$ exhibits several cusplike features. These reflect the fact that different quasiparticles in the same multiplet have different velocities. Notice that these cusplike features could be detected in numerical studies by monitoring the behavior of $dI_3/dt$, similar to what observed for the von Neumann entropy [2].

## VI. ISING CHAIN WITH STAGGERED TRANSVERSE MAGNETIC FIELD

Here we derive the quasiparticle picture for $I_3$ after a quench in the transverse field Ising chain with staggered magnetic field [cf. Eqs. (7) and (8)]. We restrict ourselves to the situation in which the magnetic field has periodicity two, with values $h = (h_o, h_e)$, where $h_o$ and $h_e$ is the magnetic field on the odd and even sites of the chain, respectively. We consider the following quench protocol. At $t = 0$, the chain is prepared in the ground state of the model with $h^0 = (h^0_o, h^0_e)$. At $t > 0$, the magnetic field is suddenly changed to $h = (h_o, h_e)$, and the system evolves with the new Hamiltonian. In the following, we show that, similarly to the $XX$ quench discussed in Sec. V, this will give rise to a negative TMI.

To find an explicit form for the two-body correlation function $\mathcal{C}(k)$ in (27) for generic magnetic fields $h$, we have to diagonalize the $4 \times 4$ matrix $\mathcal{H}_k$ in (16) for both $h$ and $h^0$, thus determining (27) via equation (21). Although it is, in principle, possible to analytically perform the

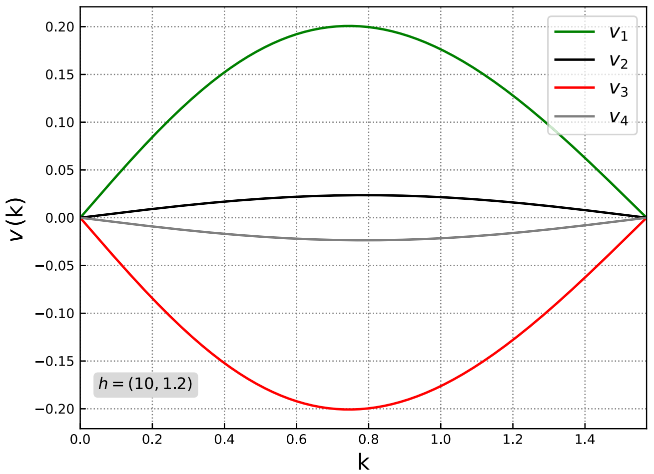


FIG. 5. Group velocities $v_j(k)$ of the quasiparticles forming entangled quadruplets in the Ising chain with $h = (10, 1.2)$. We plot $v_j(k)$ versus the quasimomentum $0 \leqslant k \leqslant \pi/2$. Notice that $v_1(k) > v_2(k) > v_4(k) > v_3(k)$ for any $k$ except at $k = 0, \pi/2$, where they all vanish.

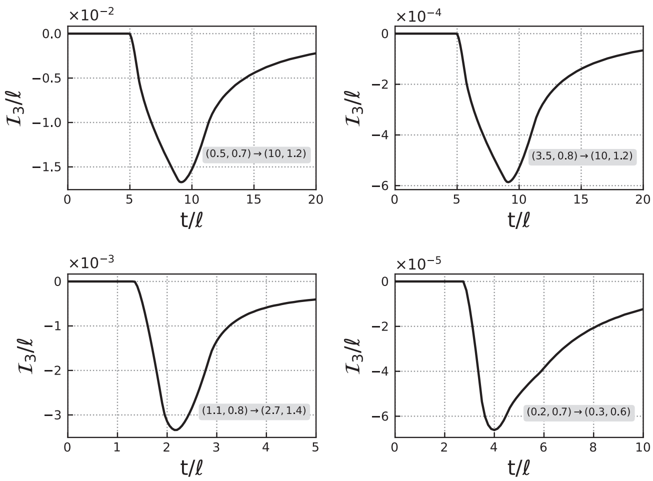


FIG. 6. Tripartite mutual information (TMI) between three adjacent intervals of length $\ell$ after a quench in the transverse field Ising chain. We plot the density $I_3/\ell$ for TMI versus the rescaled time $t/\ell$. The different panels correspond to different quenches $(h_o^0, h_e^0) \to (h_o, h_e)$. Notice that the $y$ axis is rescaled, the rescaling factor being reported at the top of each panel.

diagonalization in our specific case of a two-site periodic field, the expressions for the eigenvalues $\varepsilon_i(k)$ and the eigenvectors as functions of $h$, $h^0$, and $k$ are very cumbersome and not particularly enlightening. Thus we prefer to perform the diagonalization numerically. From the eigenvalues $\varepsilon_i(k)$, one obtains the group velocities of the quasiparticles as $v_i(k) = d\varepsilon_i(k)/dk$. For the following, it is useful to observe that $v_i(k) = -v_{i+n}(k)$, because the eigenvalues of $\mathcal{H}_k$ are organized in pairs with opposite signs [see Eq. (20)]. In Fig. 5, we report the group velocities $v_j(k)$ for the Ising chain with $n = 2$ and $h = (10, 1.2)$. The quasimomentum $k$ of the species is in $[0, \pi/2]$. Notice that the order of the velocities associated to the various quasiparticle species is the same for all the quasimomenta. The same holds for all the values of $h$ we take into account in the following. This means that the kinematics of the quasiparticles is qualitatively the same as in the $XX$ chain after the quench discussed in Sec. V, and we have the same scenario as in Fig. 3. In the hydrodynamic limit, $I_3$ is thus described by the formula

$$I_3(t) = \int_0^{\pi/2} \frac{dk}{2\pi} \tau_3(k)(\mathcal{D}_1(k, \ell, t) + \mathcal{D}_2(k, \ell, t)), \qquad (61)$$

where the functions $\mathcal{D}_1$ and $\mathcal{D}_2$ are the same as in (60) if we label the quasiparticle species so that $v_1 > v_2$. Here the entanglement content $\tau_3(k)$ is the same as in (45), where $s_{\{x\}}(k)$ is the entropy obtained numerically from $\mathcal{C}(k)$ [cf. Eq. (27)] as explained in Sec. III. Clearly, now $\tau_3$ depends on $k$, in contrast with the case of the $XX$ chain (see Sec. V).

In Fig. 6, we show the quasiparticle prediction for $I_3$ in the Ising chain after several quenches $h^{(0)} \to h$ (different panels in the figure). The results are for three adjacent intervals of equal length $\ell$. Again, the quasiparticle picture holds in the hydrodynamic limit $\ell, t \to \infty$ with the ratio $t/\ell$ fixed. Interestingly, for all the quenches that we analyzed the TMI attains quite "small" values $\lesssim 10^{-2}$. The TMI is zero at short times. Precisely, one has $I_3/\ell = 0$ for $t/\ell \leqslant 1/v_{\max}$. As it is clear from Fig. 5 one has $v_{\max} \approx 0.2$ for the quench with $h = (10, 1.2)$, which implies that $I_3 = 0$ for $t/\ell \lesssim 5$. At $t/\ell = 1/v_{\max}$, the TMI starts decreasing. This happens because an entangled quadruplet created at the boundary between $A_1$ and $A_2$ (or $A_2$ and $A_3$) starts to be shared, and hence it contributes to $I_3$. Quite generically, at later times $I_3$ is negative, and becomes smaller and smaller upon increasing times. Thus $I_3$ reaches a minimum, and then starts growing. At asymptotically long times $I_3$ vanishes. The vanishing of the TMI signals that, although the multiplets exhibit nontrivial correlations, the dynamics of the quantum information shared between the different intervals happens in a "localized" manner via the propagation of the quasiparticles. The vanishing of $I_3$ reflects that at infinite times there are no entangled quadruplets that are shared between $A_1$, $A_2$, and $A_3$ and the complement of $A$.

## VII. NUMERICAL BENCHMARKS

In this section, we benchmark our predictions (60) and (61) against numerical simulations. Again, we focus on the hydrodynamic limit. In Sec. VII A we discuss the case of the $XX$ chain, whereas in Sec. VII B, we consider the Ising chain. In both sections, we consider the situation with three adjacent intervals $A_1$, $A_2$, and $A_3$ of equal length $\ell$. We discuss data for $\ell \lesssim 400$. Our numerical results for the TMI in the $XX$ chain are obtained by using (27) where $F_{ij} = 0$ and $G_{ij}$ is given in (53). The starting point is the real space correlator $\mathcal{C}$ for the full chain, which satisfies a system of $L^2$ linear differential equations. These equations can be efficiently solved, for instance by Fourier transform, allowing one to obtain the dynamics of the correlator. From that, one can obtain the von Neumann entropy of any subsystem at any time by using the method of Ref. [49]. The calculation of the TMI is then straightforward by using (1). A similar, although slightly more involved, procedure can be employed for the Ising chain.

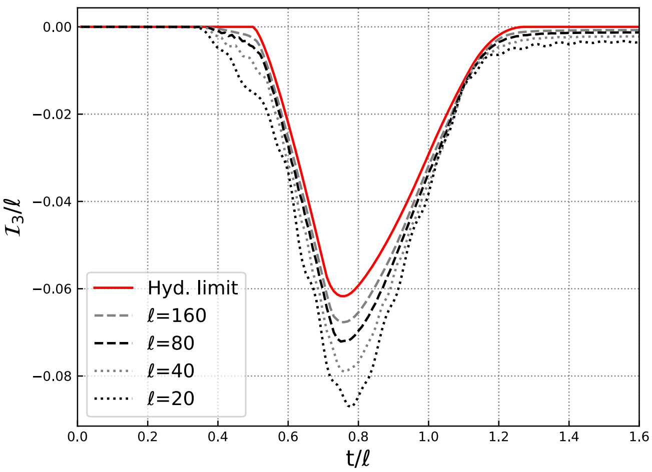


FIG. 7. Dynamics of the tripartite mutual information $I_3$ in the $XX$ chain after the quench from the state $|\Phi_0\rangle$ [cf. Eq. (15)]. We show results in the hydrodynamic limit. The different lines are for different lengths $\ell$ of the intervals. The continuous line (red line) is the prediction of the quasiparticle picture (60).

### A. $XX$ chain

Our numerical results for the $XX$ chain are reported in Fig. 7. The figure shows numerical data for $I_3/\ell$ plotted as a function of $t/\ell$. The initial state of the quench is $|\Phi_0\rangle$ [cf. Eq. (15)]. Fig. 7 shows that even for finite $\ell$ the TMI is negative at all times. However, deviations from the quasiparticle picture [cf. Eq. (60) and continuous red line in Fig. 7] are visible. Upon increasing $\ell$ the numerical data approach the analytic result. A more systematic analysis is reported in Fig. 8 where we show data for $(I_3^{(th)} - I_3)/\ell$ at fixed $t/\ell = 0.7$ and $t/\ell = 1.1$ plotted versus $1/\ell$. We show data for $\ell \lesssim 400$.

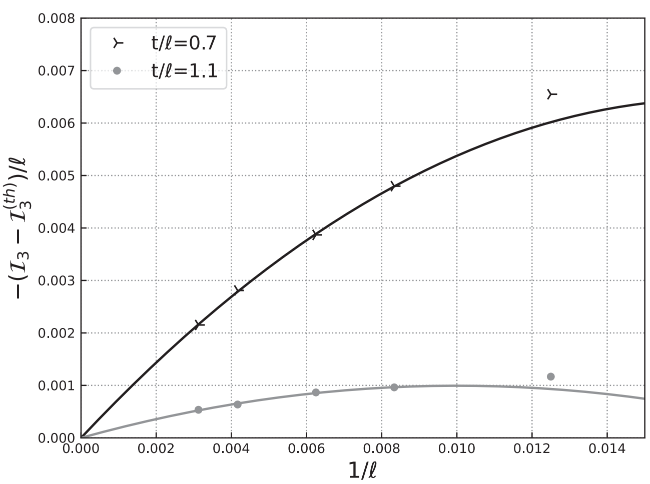


FIG. 8. Dynamics of $I_3$ after the quench from the state $|\Phi_0\rangle$ in $XX$ chain. Finite-size corrections to the hydrodynamic limit. The figure shows the difference $(I_3 - I_3^{(th)})/\ell$, with $I_3^{(th)}$ being the quasiparticle prediction for $I_3$ in the hydrodynamic limit. The $x$ axis shows $1/\ell$, with $\ell$ being the length of the intervals. The symbols in the figure are the results at fixed $t/\ell$. The full lines are fits to $a/\ell + b/\ell^2$, with $a, b$ fitting parameters. For both values of $t/\ell$ the rightmost point is excluded from the fit.

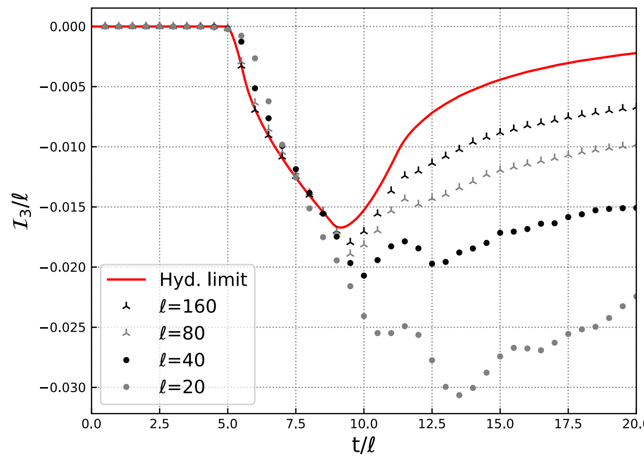


FIG. 9. Dynamics of $I_3$ after a quench in the Ising chain with staggered transverse field. Here we consider the quench $h^{(0)} = (0.5, 0.7) \to h = (10, 1.2)$. The figure shows $I_3/\ell$ for the geometry with three adjacent intervals of equal size $\ell$ (see Fig. 1). The continuous red line is the prediction in the hydrodynamic limit, equation (61). Notice that at finite $\ell$ the data exhibits strong oscillating corrections.

Here $I_3^{(3)}$ is (60). The continuous lines in Fig. 8 are fits to $a/\ell + b/\ell^2$, with $a, b$ fitting parameters. The functional form of the fitting function is motivated by the fact that similar corrections are observed for the von Neumann entropy [2]. Moreover, such corrections appear naturally in the stationary phase approximation [50] that is used to derive (60).

### B. Ising chain

Let us now discuss the behavior of $I_3$ after a quench in the Ising chain with staggered magnetic field (see Sec. II). Here we consider the case with $h^{(0)}$ and $h$ taking different values on the odd and even sites of the lattice. The quench protocol is as follows. The chain is initially prepared in the ground state of the Ising chain with $h^{(0)}$. At $t = 0$ the magnetic field is suddenly quenched to the final value $h$, and the system evolves with the new Hamiltonian.

In Fig. 9, we show numerical results for $I_3$ for the quench $(0.5, 0.7) \to (10, 1.2)$. Now, the finite-size data exhibit sizable deviations from the analytic result in the hydrodynamic limit (reported as continuous red curve in Fig. 9). Moreover, the data show a clear oscillating behavior as a function of time. Still, upon increasing $\ell$ the numerical results approach the analytic curve. In Fig. 10, we perform a finite-size scaling analysis plotting $I_3^{(th)} - I_3$, where $I_3^{(th)}$ is the hydrodynamic formula (61). As for the $XX$ chain (see Fig. 8), the continuous lines are fits to $a/\ell + b/\ell^2$. The quality of the fits is satisfactory, confirming the validity of (61).

## VIII. CONCLUSIONS

We derived a quasiparticle picture description for the dynamics of the tripartite information after quantum quenches in the $XX$ chain and the Ising chain with staggered magnetic field. Precisely, we focused on the situation in which entangled multiplets are produced after the quench. In the

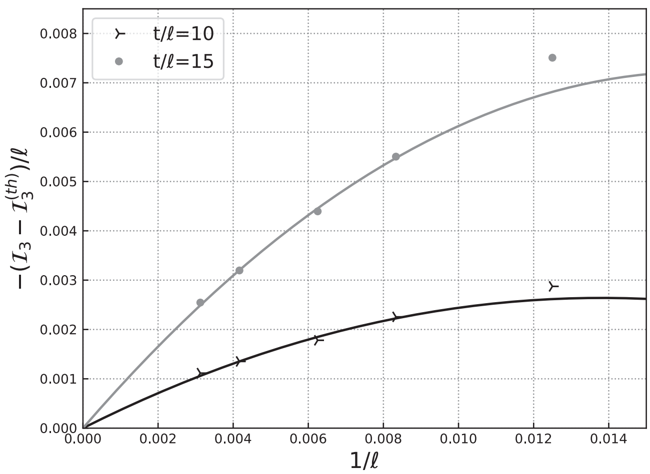


FIG. 10. Dynamics of $I_3$ after a magnetic field quench in the transverse field Ising chain. The setup is the same as in Fig. 9. We show the finite-size corrections to $I_3$ plotting $I_3^{(th)} - I_3$, with $I_3^{(th)}$ given by (61), versus $1/\ell$ at fixed $t/\ell = 10$, 15. The continuous lines are fits to $q/\ell + b/\ell^2$, with $a$, $b$ fitting parameters. For both values of $t/\ell$ the rightmost point is excluded from the fit.

presence of entangled pairs (or triplets) of quasiparticles, the TMI vanishes in the hydrodynamic limit of long times and large subsystems, with their ratio fixed. Instead, if entangled multiplets with more than three particles are present, the TMI is nonzero. Moreover, for the entangled multiplets investigated in Ref. [11] the TMI is positive at intermediate times. This reflects that the quasiparticles forming the entangled multiplets are only "classically" correlated, and the dynamics of the von Neumann entropy and of the TMI are describable in terms of GGE thermodynamic information [11]. In contrast, we showed that if the quasiparticles forming the entangled multiplets are nontrivially correlated, the TMI is negative at intermediate times. In the latter case, a hydrodynamic description of the TMI is still possible. However, the correlation content of the multiplets is not given in terms of the GGE, although it can be determined with modest computational cost for systems that are mappable to free fermions. The relationship between the entanglement content and the GGE is recovered only in the limit of long times, $t/\ell \to \infty$, when the distance between the quasiparticles forming a multiplet is large, and only one quasiparticle can be in the subsystem.

Our work opens several interesting research avenues. First, it is important to further investigate the relationship between the sign of the TMI and the structure of the entangled multiplets. Specifically, it would be interesting to understand under which conditions on the fermionic correlation matrix (27) the TMI is negative. While we showed that genuine quantum correlation between the quasiparticles forming the multiplets is necessary to have negative TMI, it is not clear whether the converse is true. It would be interesting to understand whether it is possible to have nontrivially entangled multiplets giving a positive TMI. Also, it would be interesting to investigate the behavior of the TMI in free-boson systems [9]. An important direction would be to extend our results to free-fermion and free-boson systems in the presence of dissipation. It has been shown [51–55] that for quadratic Markovian dissipative dynamics it is possible to employ the quasiparticle picture to describe the dynamics of entanglement-related quantities. Unfortunately, so far only quenches giving rise to entangled pairs were explored. It would be interesting to understand whether the dissipative quasiparticle picture can be generalized to the case of entangled multiplets. A crucial question is how dissipative processes affect the TMI. Furthermore, it is of paramount importance to understand the effect of interactions, although this is a formidable task. A possibility is to study the dynamics from (15) in the $XXZ$ spin chain, which is interacting. However, it is not clear that the dynamics ensuing from (15) can be described in terms of multiplets. Moreover, to build a quasiparticle picture for the TMI, or even for the entanglement entropy, one has to determine the correlations between the quasiparticles forming the multiplet, which is a nontrivial task. Finally, it would be interesting to understand to which extent it is possible to recover the quasiparticle picture from the ballistic fluctuation theory [56] in the presence of entangled multiplets.

## ACKNOWLEDGMENTS

We would like to thank P. Ruggiero for bringing to our attention Ref. [12] and for discussions. We would also like to thank F. Carollo for discussions in a related project.

## APPENDIX A: SINGLE-INTERVAL ENTROPY IN THE PRESENCE OF QUADRUPLETS: AN *AB INITIO* DERIVATION

In the following, we provide an *ab initio* derivation of the quasiparticle picture for the von Neumann entropy of an interval $A$ embedded in an infinite system after the quench from $|\Phi_0\rangle$ [cf. Eq. (15)] in the $XX$ chain.

Specifically, we consider the von Neumann entropy of an interval of size $\ell$ at a time $t$ after the quench. We consider the hydrodynamic limit.

The computation of the entropy of a subsystem $A$ for a Gaussian fermionic state with well-defined particle number relies on the well-known formula

$$S_A = -\mathrm{Tr}[G_A \ln(G_A) + (\mathbb{1} - G_A)\ln(\mathbb{1} - G_A)], \tag{A1}$$

where the matrix $G$ is the two-point fermionic correlation function in the real space

$$G_{x,y}(t) = \mathrm{Tr}[c_x^\dagger c_y \rho(t)] = \langle\Phi_0|e^{iHt}c_x^\dagger c_y e^{-iHt}|\Phi_0\rangle, \tag{A2}$$

and the subscript $A$ is to stress that we restrict to subsystem $A$. To obtain the hydrodynamic limit of (A1), we start from the moments $\mathrm{Tr}[G_A^n]$. By knowing the analytic dependence on $n$ of the moments, it is possible to obtain the hydrodynamic limit of (A1).

First, the matrix elements (A2) are obtained by using the Fourier transform (5) as

$$\begin{aligned} G_{x,y}(t) &= \frac{1}{L}\sum_{k,p}\langle\Phi_0|c_k^\dagger c_p|\Phi_0\rangle e^{i(kx-py)}e^{i(\varepsilon(k)-\varepsilon(p))t} \\ &= \frac{1}{L}\sum_{k,j}\langle\Phi_0|c_k^\dagger c_{p_j(k)}|\Phi_0\rangle \\ &\quad\times e^{i[kx-(k-\frac{\pi}{2}j)y]}e^{i[\varepsilon(k)-\varepsilon(k-\frac{\pi}{2}j)]t}, \end{aligned} \tag{A3}$$

where $k$ is the quasimomentum, $\varepsilon(k)$ is the dispersion of the $XX$ chain [cf. Eq. (6)], and $j = 0,\ 1,\ 2,$ and 3. In (A3), we exploited the *four*-site translation invariance of $|\Phi_0\rangle$, which implies that $\langle\Phi_0|c_k^\dagger c_p|\Phi_0\rangle \neq 0$ only when $4(k-p)$ is an integer multiple of $2\pi$. Indeed, in (A3), we defined $p_j(k)$ as the quasimomentum in $(-\pi,\pi]$ such that $k - p_j(k) = j\frac{\pi}{2} \mod 2\pi$.

The expectation value in (A3) $\langle\Phi_0|c_k^\dagger c_{p_j(k)}|\Phi_0\rangle$ is given in (53). Thus, in the thermodynamic limit $L \to \infty$, we can rewrite (A3) as

$$G_{x,y} = \int_{-\pi}^{\pi} \frac{dk}{2\pi} e^{ik(x-y)} \left[ \frac{1}{2} - i^y \frac{1+i}{4} e^{it(\varepsilon(k)-\varepsilon(k-\frac{\pi}{2}))} - (-i)^y \frac{1-i}{4} e^{it(\varepsilon(k)-\varepsilon(k-\frac{3\pi}{2}))} \right]. \tag{A4}$$

It is convenient to exploit explicitly the four-site periodicity of (A4), defining the block matrix $\Gamma_{x,y}$ as

$$\Gamma_{x,y}(t) := G_{4x+i,4y+j} = \frac{1}{2} \int_{-\pi}^{\pi} \frac{dk}{2\pi} e^{4ik(x-y)} \Gamma_k, \tag{A5}$$

where $\Gamma_k$ is defined as

$$\Gamma_k := \mathbb{1}_4 + \Gamma_k^{(1)} e^{it(\varepsilon(k)-\varepsilon(k-\frac{\pi}{2}))} + \Gamma_k^{(2)} e^{it(\varepsilon(k)-\varepsilon(k-\frac{3\pi}{2}))}, \tag{A6}$$

and $\mathbb{1}_4$ is the $4\times 4$ identity matrix, and we defined $\Gamma_k^{(1)}$ and $\Gamma_k^{(2)}$ as

$$\Gamma_k^{(1)} = \frac{1}{2} \begin{pmatrix} 1-i & (1+i)e^{-ik} \\ (1-i)e^{ik} & 1+i \end{pmatrix} \otimes \begin{pmatrix} 1 & -e^{-2ik} \\ e^{2ik} & -1 \end{pmatrix} = \frac{1}{2}\left(\mathbb{1}_2 + \sigma_x^{(k)} - \sigma_y^{(k)} - i\sigma_z^{(k)}\right) \otimes \left(\sigma_z^{(2k)} - i\sigma_y^{(2k)}\right). \tag{A7}$$

We also defined

$$\Gamma_k^{(2)} = \frac{1}{2} \begin{pmatrix} 1+i & (1-i)e^{-ik} \\ (1+i)e^{ik} & 1-i \end{pmatrix} \otimes \begin{pmatrix} 1 & -e^{-2ik} \\ e^{2ik} & -1 \end{pmatrix} = \frac{1}{2}\left(\mathbb{1}_2 + \sigma_x^{(k)} + \sigma_y^{(k)} + i\sigma_z^{(k)}\right) \otimes \left(\sigma_z^{(2k)} - i\sigma_y^{(2k)}\right). \tag{A8}$$

In (A7) and (A8), we introduced the rotated Pauli matrices $\sigma_\alpha^{(k)}$ as

$$\sigma_\alpha^{(k)} = e^{-i\frac{k}{2}\sigma_z}\ \sigma_\alpha\ e^{i\frac{k}{2}\sigma_z}. \tag{A9}$$

Let us define the functions $f_1(k)$, $f_2(k)$, and $g(k)$ as

$$f_1(k) := \mathbb{1}_2 + \sigma_x^{(k)} - \sigma_y^{(k)} - i\sigma_z^{(k)}, \tag{A10}$$

$$f_2(k) := \mathbb{1}_2 + \sigma_x^{(k)} + \sigma_y^{(k)} + i\sigma_z^{(k)}, \tag{A11}$$

$$g(k) := \sigma_z^{(2k)} - i\sigma_y^{(2k)}. \tag{A12}$$

Now, to evaluate $\mathrm{Tr}[G_A^n]$, one has to trace over the indices $x, y$ of the $\Gamma_{x,y}$ and also over products of the $4\times 4$ blocks introduced in (A5). The first trace can be performed by exploiting the identity

$$\sum_{z=1}^{\ell/4} e^{4izk} = \frac{\ell}{8} \int_{-1}^{1} d\xi\ w([k]_{\pi/2}) e^{i(\ell\xi+\ell+4)[k]_{\pi/2}/2}, \tag{A13}$$

where

$$w(k) := \frac{2k}{\sin(2k)}. \tag{A14}$$

The notation $[k]_{\pi/2}$ in (A13) means that the quasimomentum $k$ is considered modulo $\pi/2$. Thus we can rewrite $\mathrm{Tr}[G_A^n]$ as

$$\mathrm{Tr}\big[G_A^n\big] = \left(\frac{\ell}{8}\right)^n \int_{-\pi}^{\pi} \frac{d^n k}{(2\pi)^n} \int_{-1}^{1} d^n\xi\ \mathrm{Tr} \prod_{j=1}^{n} \Gamma_{k_j} \times \prod_{j=1}^{n} w([k_j - k_{j-1}]_{\pi/2}) e^{i(\ell\xi_j+\ell+4)[k_j-k_{j-1}]_{\pi/2}/2}, \tag{A15}$$

where $\Gamma_k$ is the $4\times 4$ block matrix introduced in (A5), and we identified $k_0 \equiv k_n$. We are interested in finding the leading term in the hydrodynamic limit. The strategy is to use the stationary phase approximation of the integral in (A15). The stationary phase approximation states that [50]

$$\lim_{\ell\to\infty} \int_\Omega d^N x\ B(\mathbf{x}) e^{i\ell A(\mathbf{x})} = \left(\frac{2\pi}{\ell}\right)^{N/2} \sum_j B(\mathbf{x_j}) |\det H(\mathbf{x_j})|^{-\frac{1}{2}} e^{i\ell A(\mathbf{x_j}) + i\pi\sigma(\mathbf{x_j})/4}, \tag{A16}$$

Here $A(\mathbf{x})$ and $B(\mathbf{x})$ are functions, and $\mathbf{x_j}$ are the stationary points of $A(\mathbf{x})$ that are in the integration domain $\Omega$. In (A16) $H$ is the Hessian matrix of $A$ and $\sigma$ is its signature, i.e., the difference between the number of positive and negative eigenvalues. We now apply (A16) to the integral on the $2n-2$ variables $k_2,\ldots,k_n,\xi_2,\ldots,\xi_n$ in (A15). The stationarity conditions $\partial_{\xi_j} A = 0$ imply that the stationary points must satisfy the equation

$$[k_j - k_1]_{\pi/2} = 0 \quad \forall j. \tag{A17}$$

This implies that $w([k_j - k_{j-1}]_{\pi/2}) = 1$ for all the stationary points.

Let us now discuss the consequences of the stationarity condition with respect to the $k_j$, i.e., $\partial_{k_j} A = 0$. Now, the analysis is more complicated because one has to take the trace of arbitrary powers of $\Gamma_k$ [cf. Eq. (A15)]. Since $\Gamma_k$ is the sum of three terms, this means that for fixed $n$ there are $3^n$ terms. Moreover, $\Gamma_k$ contains phase factors which have to be treated carefully in the stationary phase approximation.

To proceed, we observe that both $\Gamma_k^{(1)}$ and $\Gamma_k^{(2)}$ contain a term $g(k)$ [cf. Eq. (A12)]. Moreover, due to the tensor product in (A7) and (A8), we can perform the trace operation on the terms with $g(k)$ separately. In the following, we discuss the conditions on $k_j$ to have a nonzero trace. We observe the following.

(i) The terms $g(k)^2$ are identically zero. Since $g(k) = g(k\pm\pi)$, the terms $g(k)g(k\pm\pi)$ are also zero.

(ii) $g(k)g(k\pm\frac{\pi}{2}) = 2(\mathbb{1}_2 + \sigma_x^{(2k)})$.

(iii) The trace of the product of an *odd* number of $g(k_i)$ with $[k_i - k_j]_{\pi/2} = 0$ is zero. Indeed, one possibility is that the product is identically zero, if two of the factors satisfy the condition in (i). The only other possibility is that the product is of the form $a\sigma_y^{(2k)} + b\sigma_z^{(2k)}$, with $a$ and $b$ constants. This is obtained by repeatedly using (ii). Again, the trace of the result is zero.

(iv) The trace of the product of an *even* number $2m$ of blocks $g(k_{j_i})$, provided that $k_{j_i} - k_{j_{i-1}} = \pm\pi/2 \bmod 2\pi$, is $2^{2m}$. This is a straightforward consequence of (ii).

In summary, the observations $(i) - (iv)$ imply that in the product $\prod_{j=1}^{n} \Gamma_{k_j}$ in (A15) only terms with an even number $2m$ of factors $\Gamma_k^{(1)}$ or $\Gamma_k^{(2)}$ [cf. Eqs. (A7) and (A8)] are not zero. The quasimomenta $k_{j_1}, \dots, k_{j_{2m}} \in (-\pi, \pi]$ associated to each $\Gamma^{(1)}$ or $\Gamma^{(2)}$ factor are such that $k_{j_i} - k_{j_{i-1}} = \pm\frac{\pi}{2} \mod 2\pi$. As discussed above, the trace over the factors $g(k)$ gives a factor $2^{2m}$. Let us now determine the contributions of the trace over the matrices $f_1$ and $f_2$ [cf. Eqs. (A10) and (A11)]. To proceed, it is straightforward to check the following properties of $f_1$ and $f_2$:

(1) $f_1(k)f_1(k+\frac{\pi}{2}) = f_1(k)f_2(k+\frac{\pi}{2}) = 0$,
(2) $f_2(k)f_1(k-\frac{\pi}{2}) = f_2(k)f_2(k-\frac{\pi}{2}) = 0$,
(3) $f_1(k)f_2(k-\frac{\pi}{2}) = f_2(k)f_1(k+\frac{\pi}{2}) = 4(\mathbb{1}_2 + \sigma_x^{(k)})$,
(4) $f_1(k)f_1(k-\frac{\pi}{2}) = -4(\sigma_y^{(k)} + i\sigma_z^{(k)})$,
(5) $f_2(k)f_2(k+\frac{\pi}{2}) = 4(\sigma_y^{(k)} + i\sigma_z^{(k)})$,
(6) $f_1(k\pm\pi)f_2(k\pm\pi-\frac{\pi}{2}) = f_2(k\pm\pi)f_1(k\pm\pi+\frac{\pi}{2}) = 4(\mathbb{1}_2 - \sigma_x^{(k)})$,
(7) $f_1(k\pm\pi)f_1(k\pm\pi-\frac{\pi}{2}) = 4(\sigma_y^{(k)} - i\sigma_z^{(k)})$,
(8) $f_2(k\pm\pi)f_2(k\pm\pi+\frac{\pi}{2}) = 4(-\sigma_y^{(k)} + i\sigma_z^{(k)})$.

The first two relations show that, to have a nonzero product, if we have a matrix $f_1$ with an associated quasimomentum $k_{j_i}$, the next matrix must have an associated quasimomentum $k_{j_{i+1}} = k_{j_i} - \frac{\pi}{2} \bmod 2\pi$, while a matrix $f_2$ with associated quasimomentum $k_{j_i}$ must be followed by a matrix with associated quasimomentum $k_{j_{i+1}} = k_{j_i} + \frac{\pi}{2} \bmod 2\pi$. Thus $f_1$ can be seen as a "lowering operator" for the quasimomentum and represented as $\searrow$. Similarly, $f_2$ can be seen as a "raising operator" and represented as $\nearrow$.

We can represent any product of $f_1$ and $f_2$ not yielding 0 as a sequence of these operators, which raise or lower the starting $k_{i_1} = k$ by $\frac{\pi}{2}$. Again, we remind that we are interested only in *even* sequences. Relations 3 and 6 are associated to the subsequences $\searrow\nearrow$ and $\nearrow\searrow$. Similarly, rules 4 and 7 are associated to the subsequence $\searrow\searrow$ and rules 5 and 8 to the subsequence $\nearrow\nearrow$.

Moreover, from the rules 3–8 it follows that only sequences with final quasimomentum equal to $k$ modulo $2\pi$ give a nonzero contribution, as an odd number of $\nearrow\nearrow$ or $\searrow\searrow$ (corresponding to a change of $\pm\pi$ in the quasimomentum) yield a product of the form $(a\sigma_y^{(k)} + b\sigma_z^{(k)})$, whose trace is zero.

Finally, we have to compute the contribution of the sequences of $f_1, f_2$ that give a nonzero result. To this purpose, let us observe the following.

(a) A subsequence $\nearrow\searrow \cdots \nearrow\searrow$ or $\searrow\nearrow \cdots \searrow\nearrow$ yields a factor $2^{3p/2-1}(\mathbb{1}_2 + \sigma_x^{(k)})$, where $p$ is the number of operators (rule 3). The same subsequence but with starting point $k \pm \pi$ gives $2^{3p/2-1}(\mathbb{1}_2 - \sigma_x^{(k)})$ (see rule 6).

(b) Subsequences of four consecutive operators of the same kind, i.e., $\nearrow\nearrow\nearrow\nearrow$ (rules 5 and 8) or $\searrow\searrow\searrow\searrow$ (rules 4 and 7), yield a factor $-2^5(\mathbb{1}_2 \pm \sigma_x^{(k)})$. The sign depends on whether the first operator is associated with a quasimomentum $k$ (giving the $+$ sign) or $k \pm \pi$ (giving the $-$ sign).

(c) Any subsequence that can be decomposed in subblocks as those described in (a) and (b) yields a factor $(-1)^w\, 2^{3p/2-1}(\mathbb{1}_2 \pm \sigma_x^{(k)})$, where $p$ is the number of operators, $w$ is the number of "windings" around the Brillouin zone of the sequence, and the sign depends on whether the first operator is associated with a quasimomentum $k$ or $k \pm \pi$, as in (b).

(d) A generic sequence cannot always be decomposed only in terms of subsequences of the type in (c). Let us consider a "maximal" subsequence of type (c) that can be identified in the main sequence (i.e., has not adjacent blocks of the form $\nearrow\searrow$, $\searrow\nearrow$, $\nearrow\nearrow\nearrow\nearrow$ or $\searrow\searrow\searrow\searrow$), and that starts from $k \pm \pi$. We represent such sequence with a $\square$. It is clear that the $\square$ must be connected to the remaining parts of the sequence as $\nearrow\nearrow \square \searrow\searrow$, $\searrow\searrow \square \nearrow\nearrow$, $\nearrow\nearrow \square \nearrow\nearrow$, or $\searrow\searrow \square \searrow\searrow$. This subsequence corresponds to a factor (see rules 4–8) $(-1)^w 2^{3p/2-1}(\mathbb{1}_2 + \sigma_x^{(k)})$, where $p$ is the number of operators, $w$ is the number of "windings" around the Brillouin zone of the subsequence. Notice that in the cases $\nearrow\nearrow \square \nearrow\nearrow$ and $\searrow\searrow \square \searrow\searrow$ the number of windings of $\square$ is raised by 1.

(e) By using rules (a)–(d), we are left with sequences of the form $\propto (\mathbb{1}_2 + \sigma_x^{(k)})$. Then, it is straightforward to realize that the contribution of *any* sequence that does not give zero (that is, those with an integer number of "windings" around the Brillouin zone) is $(-1)^w\, 2^{3p/2}$, where $p = 2m$ is the (even) number of operators and $w$ the number of windings.

The result in (e) allows us to write an expression that generates the contributions of all the sequences. Indeed, if we associate $f_1 \leftrightarrow \searrow \leftrightarrow 2\sqrt{2}e^{-i\frac{\pi}{4}}$ and $f_2 \leftrightarrow \nearrow \leftrightarrow 2\sqrt{2}e^{i\frac{\pi}{4}}$, we obtain that the total contribution of the sequences with $p = 2m$ factors is given by

$$\mathrm{Tr}(f_1 + f_2)^p = 2^{\frac{3p}{2}} \mathrm{Re}[(e^{-i\frac{\pi}{4}} + e^{i\frac{\pi}{4}})^p]. \tag{A18}$$

In (A18) we used that at any stationary point that gives a nonzero contribution the oscillating factors that are present in the rotated Pauli matrices [cf. Eq. (A9)] cancel out.

Let us now proceed to determine the consequences of the stationarity conditions with respect to $k_j$. The generic term originating from the product $\prod_{j=1}^{n} \Gamma_{k_j}$ [cf. Eq. (A5)] contains $f_1(k_j)$, $f_2(k_j)$, or the identity. In the last case, the quasimomentum $k_j$ does not appear. Stationarity with respect to the missing quasimomenta $k_j$ imply that

$$\ell(\xi_j - \xi_{j+1}) = 0 \;\Rightarrow\; \xi_j = \xi_{j+1}. \tag{A19}$$

Instead, for the quasimomenta $k_{j_1}, \dots, k_{j_m}$ that appear in the block, the stationarity condition yields

$$\ell(\xi_{j_i} - \xi_{j_i+1}) + t\left[v(k_{j_i}) - v\left(k_{j_i} \pm \frac{\pi}{2}\right)\right] = 0 \Rightarrow \ell\xi_{j_i} + v(k_{j_i})t = \ell\xi_{j_{i+1}} + v(k_{j_{i+1}})t \;\forall i. \tag{A20}$$

In (A20), we used that $\xi_{j_i+1} = \xi_{j_{i+1}}$, which follows from (A19) applied to the $\xi_l$ with $j_i < l < j_{i+1}$. Moreover, the condition to have a nonzero trace implies that $k_{j_i} \pm \frac{\pi}{2} = k_{j_{i+1}}$. The conditions (A19) and (A20) give some nontrivial constraints on the stationary value of $\xi_1 = \xi_{j_m}$. The constraint is determined by the condition that all the $\xi_j \in [-1, 1]$. Let us define $k := k_{j_n}$. The result depends on the remaining quasimomenta in the string of operators $\Gamma_{k_j}$.

We can distinguish three families of quasimomenta $k_{j_i}$.

($\alpha$) The quasimomenta in the string take only the values $k, k+\frac{\pi}{2}$ or $k, k-\frac{\pi}{2}$.

($\beta$) The quasimomenta $k_{j_i}$ take only three of the four values $k, k+\frac{\pi}{2}, k-\frac{\pi}{2}, k\pm\pi$.

($\gamma$) The quasimomenta $k_{j_i}$ take all the four values $k, k+\frac{\pi}{2}, k-\frac{\pi}{2}, k\pm\pi$.

Now, one can verify that for case ($\alpha$), Eq. (A20) implies the condition

$$\xi_{j_i}=\xi_1+\left[v(k)-v\left(k\pm\frac{\pi}{2}\right)\right]\frac{t}{\ell}\in[-1,1]. \tag{A21}$$

Thus the integration over $\xi_1$ gives the function $M_1(k)$

$$M_1(k)=\max\left\{0,2-\left|v(k)-v\left(k\pm\frac{\pi}{2}\right)\right|\frac{t}{\ell}\right\}, \tag{A22}$$

where $v(k)=2\sin(k)$. For the second case ($\beta$), without loss of generality we can choose $k$ to be the smaller of the three quasimomenta present. The constraints from (A20) now read

$$\xi_{j_i}=\xi_1+\left[v(k)-v\left(k+\frac{\pi}{2}\right)\right]\frac{t}{\ell}\in[-1,1], \tag{A23}$$

$$\xi_{j_j}=\xi_1+[v(k)-v(k+\pi)]\tfrac{t}{\ell}\in[-1,1]. \tag{A24}$$

By integrating over $\xi_1$, a straightforward but tedious calculation yields

$$M_2(k)=\max\left\{0,2-\max\left\{\left|v(k)-v\left(k+\frac{\pi}{2}\right)\right|,\right.\right.$$
$$\left.\left.|v(k)-v(k+\pi)|,\left|v(k)+v\left(k+\frac{\pi}{2}\right)\right|\right\}\frac{t}{\ell}\right\}. \tag{A25}$$

Finally, in the third case ($\gamma$), we have three constraints like those in Eqs. (A22) and (A23). Specifically, we obtain

$$M_3(k)=\max\{0,2-\max\{|v(k)-v(k+\pi)|,$$
$$\left.\left.\left|v\left(k-\frac{\pi}{2}\right)+v\left(k+\frac{\pi}{2}\right)\right|\right\}\frac{t}{\ell}\right\}. \tag{A26}$$

Before putting everything together, we notice that for the stationary points that give a nonzero contribution we have $|\det H(\mathbf{x_j})|=(\frac{1}{2})^{2n-2}$ and $\sigma(\mathbf{x_j})=0$ [cf. Eq. (A16)]. Finally, we obtain

$$\mathrm{Tr}\left[G_A^n\right]=\frac{\ell}{16^n}\int_{-\pi}^{\pi}\frac{dk}{2\pi}\,2^{n-1}\left\{2\cdot4^n+\sum_{m=1}^{\lfloor\frac{n}{2}\rfloor}\binom{n}{2m}4^{n-2m}\left(\frac{1}{2}\right)^{2m}2^{2m}\cdot2^{3m}\left[2M_1(k)+4\sum_{j=1}^{\lfloor\frac{m}{2}\rfloor}\binom{m}{2j}M_2(k)\right.\right.$$
$$\left.\left.+\left(\left(e^{i\frac{\pi}{4}}+e^{-i\frac{\pi}{4}}\right)^{2m}-2-4\sum_{j=1}^{\lfloor\frac{m}{2}\rfloor}\binom{m}{2j}\right)M_3(k)\right]\right\}, \tag{A27}$$

where $M_1,\ M_2,$ and $M_3$ are the kinematic terms (A22), (A25), and (A26). Let us explain the various combinatorial factors in (A27). The powers of 4 account for the four choices $k\pm\pi/2, k\pm\pi$ that one has for the quasimomenta that are missing in the string $\Gamma_{k_{j_1}}\Gamma_{k_{j_2}}\cdots\Gamma_{k_{j_n}}$. The missing quasimomenta are obtained by selecting $\mathbb{1}_4$ in (A5). For instance, the term $2\times4^n$ in (A27) is the contribution in which all the $\Gamma_{k_j}$ are replaced by $\mathbb{1}_4$. Notice that the factor 2 in $2\cdot4^n$ comes from the integral over $\xi_1$. The binomial $\binom{n}{2m}$ in the second term in (A27) counts the possible ways to choose an even subsequence of $\Gamma_{k_{j_1}}\Gamma_{k_{j_2}}\cdots\Gamma_{k_{j_{2m}}}$. Each of them gives a factor $\frac{1}{2}$ [cf. Eq. (A5)]. Moreover, there is a factor $2^{2m}$ and $2^{3m}$ from the trace in rule ($iv$) and from (A18), respectively. Let us now discuss the term within the square brackets in (A27). The three terms in the square brackets corresponds to the three cases ($\alpha,\beta,\gamma$). The first term corresponds to case ($\alpha$), in which the quasimomenta in the string can have only the values $k\pm\pi/2$. Now, there are only the two cases ($\nearrow\searrow\cdots\nearrow\searrow$ and $\searrow\nearrow\cdots\searrow\nearrow$) to consider, each of them giving 1, and the factor $M_1(k)$. The second term in the square brackets corresponds to case ($\beta$), in which we have configurations with an even number $2j$ of (alternated) pairs $\searrow\searrow$ and $\nearrow\nearrow$, univocally connected by subsequences of the type (a). Each configuration contributes with 1, and we have $4\sum_{j=1}^{\lfloor\frac{m}{2}\rfloor}\binom{m}{2j}$ of such configurations. The summation accounts for the ways where to place the pairs $\searrow\searrow$ and $\nearrow\nearrow$ after the string of $2m$ operators has been divided in $m$ slots of two. Moreover, the partition of the string of operators can be done by starting from even or odd sites of the string, which gives a factor 2. Besides that, there is another factor 2, coming from the fact that one can put either $\searrow\searrow$ or $\nearrow\nearrow$ in the first chosen slot, the others being filled accordingly. Finally, the remaining contributions are obtained by subtracting the cases described above from the total $(e^{i\frac{\pi}{4}}+e^{-i\frac{\pi}{4}})^{2m}$ [see Eq. (A18)]. It is now straightforward to simplify equation (A27) to obtain

$$\mathrm{Tr}\left[G_A^n\right]=\frac{\ell}{2}+\ell\int_{-\pi}^{\pi}\frac{dk}{2\pi}\left\{\left[2\left(\frac{1}{2}\right)^n-\left(\frac{2+\sqrt{2}}{4}\right)^n-\left(\frac{2-\sqrt{2}}{4}\right)^n\right]m_1(k,t)\right.$$
$$+\left[2\left(\frac{2+\sqrt{2}}{4}\right)^n+2\left(\frac{2-\sqrt{2}}{4}\right)^n-2\left(\frac{1}{2}\right)^n-1\right]m_2(k,t)$$
$$\left.+\left[\frac{1}{2}+\left(\frac{1}{2}\right)^n-\left(\frac{2+\sqrt{2}}{4}\right)^n-\left(\frac{2-\sqrt{2}}{4}\right)^n\right]m_3(k,t)\right\}, \tag{A28}$$

where we have defined

$$m_1(k,t)=\min\left\{1,\frac{t}{\ell}\left|v(k)-v\left(k+\frac{\pi}{2}\right)\right|\right\}, \tag{A29}$$

$$m_2(k,t) = \min\left\{1, \frac{t}{\ell}\max\left\{\left|v(k) - v\left(k+\frac{\pi}{2}\right)\right|, |v(k)-v(k+\pi)|, \left|v(k)-v\left(k-\frac{\pi}{2}\right)\right|\right\}\right\}, \tag{A30}$$

$$m_3(k,t) = \min\left\{1, \frac{t}{\ell}\max\left\{|v(k)-v(k+\pi)|, |v\left(k-\frac{\pi}{2}\right) - v\left(k+\frac{\pi}{2}\right)|\right\}\right\}. \tag{A31}$$

Having the hydrodynamic prediction for $\mathrm{Tr}[G_A^n]$ for any $n$ allows us to obtain the prediction for the von Neumann entropy $S_A$. The strategy is to write $S_A = \mathrm{Tr} f(G_A)$, with $f(x)$ as defined in (49). After expanding $f(x)$ around $x=0$, and using (A28) together with $f(0)=f(1)=0$ and $f(x)=f(1-x)$), we obtain

$$\begin{aligned}S_A(t) = \ell\int_{-\pi}^{\pi}\frac{dk}{2\pi}\Bigg[&\left(2f\left(\frac{1}{2}\right) - 2f\left(\frac{2+\sqrt{2}}{4}\right)\right)m_1(k,t) + \left(4f\left(\frac{2+\sqrt{2}}{4}\right) - 2f\left(\frac{1}{2}\right)\right)m_2(k,t)\\ &+\left(f\left(\frac{1}{2}\right) - 2f\left(\frac{2+\sqrt{2}}{4}\right)\right)m_3(k,t)\Bigg].\end{aligned} \tag{A32}$$

Let us now show that the *ab initio* result (A32) coincides with the result obtained from the method introduced in Sec. III. The latter approach yields

$$\begin{aligned}S_A(t) = \int_{\pi/2}^{3\pi/4}\frac{dk}{2\pi}&\{(s_{\{1\}}+s_{\{3\}})[(v_1-v_2)t\ \Theta(\ell-(v_1-v_2)t) + \ell\Theta((v_1-v_2)t-\ell) + (v_4-v_3)t\ \Theta(\ell-(v_1-v_3)t)\\ &+(\ell-(v_1-v_4)t)\chi(\ell/(v_1t-v_3t), \ell/(v_1t-v_4t))] + (s_{\{2\}}+s_{\{4\}})[((v_1-v_4)t-\ell)\chi\big(\ell/(v_1t-v_4t),\\ &\times\ \min\{\ell/(v_1t-v_2t), \ell/(v_2t-v_4t)\}\big)(v_1-v_2)t\chi(\ell/(v_2t-v_4t), \ell/(v_1t-v_2t))\\ &+(v_2-v_4)t\chi(\ell/(v_1t-v_2t), \ell/(v_2t-v_4t)) + \ell\Theta(t-\max\{\ell/(v_1t-v_2t), \ell/(v_2t-v_4t)\})]\\ &+(s_{\{1,2\}}+s_{\{3,4\}})[(v_2-v_4)t\Theta(\ell-(v_1-v_4)t) + (\ell-(v_1-v_2)t) + \chi(\ell/(v_1t-v_4t), \ell/(v_1t-v_2t))]\\ &+s_{\{1,3\}}[((v_1-v_3)t-\ell)\chi(\ell/(v_1t-v_3t), \ell/(v_1t-v_3t)) + (\ell-(v_2-v_4)t)\chi(\ell/(v_1t-v_4t), \ell/(v_2t-v_4t))]\\ &+\int_{3\pi/4}^{\pi}\frac{dk}{2\pi}\{1\leftrightarrow 2, 3\leftrightarrow 4\}.\end{aligned} \tag{A33}$$

Here $\Theta(x)$ is the Heaviside theta function, and $\chi(a,b)$ is the characteristic function of the interval $[a,b]$, with the caveat that if $b<a$, it is zero. In (A33), we dropped the dependence of the velocities on $k$ for the sake of clarity. The first term in (A33) corresponds to the situation with quasiparticle 1 or 3 in subsystem $A$ or $\bar{A}$. The second term describes the case with quasiparticles 2 or 4 in $A$ or $\bar{A}$. The third and fourth terms take into account the situations with two quasiparticles in $A$ and two in $\bar{A}$. The last term in (A33) is obtained from the previous ones by exchanging $1\leftrightarrow 2$ and $3\leftrightarrow 4$. To proceed, we determine the contributions $s_{\{x\}}$ in (A33). These are obtained from (53) by using the strategy described in Sec. III. A straightforward calculation gives $s_{\{1\}}=s_{\{2\}}=s_{\{3\}}=s_{\{4\}}=f(1/2)$, $s_{\{1,2\}}=s_{\{3,4\}}=2f((2+\sqrt{2})/4)$, $s_{\{1,3\}}=2f(1/2)$. Now, it is straightforward, although tedious, to check that (A33) is exactly the same as (A32).


[1] P. Calabrese and J. Cardy, Evolution of entanglement entropy in one-dimensional systems, J. Stat. Mech.: Theory Exp. (2005) P04010.

[2] M. Fagotti and P. Calabrese, Evolution of entanglement entropy following a quantum quench: Analytic results for the $XY$ chain in a transverse magnetic field, Phys. Rev. A **78**, 010306(R) (2008).

[3] V. Alba and P. Calabrese, Entanglement and thermodynamics after a quantum quench in integrable systems, Proc. Natl. Acad. Sci. USA **114**, 7947 (2017).

[4] B. Bertini, K. Klobas, V. Alba, G. Lagnese, and P. Calabrese, Growth of Rényi entropies in interacting integrable models and the breakdown of the quasiparticle picture, Phys. Rev. X **12**, 031016 (2022).

[5] V. Alba, B. Bertini, M. Fagotti, L. Piroli, and P. Ruggiero, Generalized-hydrodynamic approach to inhomogeneous quenches: Correlations, entanglement and quantum effects, J. Stat. Mech.: Theory Exp. (2021) 114004.

[6] P. Calabrese, F. H. L. Essler, and G. Mussardo, Introduction to 'quantum integrability in out of equilibrium systems', J. Stat. Mech.: Theory Exp. (2016) 064001.

[7] L. Vidmar and M. Rigol, Generalized Gibbs ensemble in integrable lattice models, J. Stat. Mech.: Theory Exp. (2016) 064007.

[8] F. H. L. Essler and M. Fagotti, Quench dynamics and relaxation in isolated integrable quantum spin chains, J. Stat. Mech.: Theory Exp. (2016) 064002.

[9] V. Alba and P. Calabrese, Entanglement dynamics after quantum quenches in generic integrable systems, SciPost Phys. **4**, 017 (2018).

[10] L. Piroli, B. Pozsgay, and E. Vernier, What is an integrable quench? Nucl. Phys. B **925**, 362 (2017).

[11] B. Bertini, E. Tartaglia, and P. Calabrese, Entanglement and diagonal entropies after a quench with no pair structure, J. Stat. Mech.: Theory Exp. (2018) 063104.

[12] A. Bastianello and P. Calabrese, Spreading of entanglement and correlations after a quench with intertwined quasiparticles, SciPost Phys. **5**, 033 (2018).

[13] L. Amico, R. Fazio, A. Osterloh, and V. Vedral, Entanglement in many-body systems, Rev. Mod. Phys. **80**, 517 (2008).

[14] P. Calabrese, J. Cardy, and B. Doyon, Entanglement entropy in extended quantum systems, J. Phys. A: Math. Theor. **42**, 500301 (2009).

[15] N. Laflorencie, Quantum entanglement in condensed matter systems, Phys. Rep. **646**, 1 (2016).

[16] A. Kitaev and J. Preskill, Topological entanglement entropy, Phys. Rev. Lett. **96**, 110404 (2006).

[17] M. Levin and X.-G. Wen, Detecting topological order in a ground state wave function, Phys. Rev. Lett. **96**, 110405 (2006).

[18] N. J. Cerf and C. Adami, Information theory of quantum entanglement and measurement, Physica D **120**, 62 (1998), Proceedings of the Fourth Workshop on Physics and Consumption.

[19] H. Casini and M. Huerta, Remarks on the entanglement entropy for disconnected regions, J. High Energy Phys. 03 (2009) 048.

[20] C. A. Agón, P. Bueno, and H. Casini, Tripartite information at long distances, SciPost Phys. **12**, 153 (2022).

[21] P. Hayden, M. Headrick, and A. Maloney, Holographic mutual information is monogamous, Phys. Rev. D **87**, 046003 (2013).

[22] M. Rangamani and M. Rota, Entanglement structures in qubit systems, J. Phys. A: Math. Theor. **48**, 385301 (2015).

[23] E. Iyoda and T. Sagawa, Scrambling of quantum information in quantum many-body systems, Phys. Rev. A **97**, 042330 (2018).

[24] A. Seshadri, V. Madhok, and A. Lakshminarayan, Tripartite mutual information, entanglement, and scrambling in permutation symmetric systems with an application to quantum chaos, Phys. Rev. E **98**, 052205 (2018).

[25] O. Schnaack, N. Bölter, S. Paeckel, S. R. Manmana, S. Kehrein, and M. Schmitt, Tripartite information, scrambling, and the role of Hilbert space partitioning in quantum lattice models, Phys. Rev. B **100**, 224302 (2019).

[26] S. Pappalardi, A. Russomanno, B. Žunkovič, F. Iemini, A. Silva, and R. Fazio, Scrambling and entanglement spreading in long-range spin chains, Phys. Rev. B **98**, 134303 (2018).

[27] P. Hayden and J. Preskill, Black holes as mirrors: quantum information in random subsystems, J. High Energy Phys. 09 (2007) 120.

[28] Y. Sekino and L. Susskind, Fast scramblers, J. High Energy Phys. 10 (2008) 065.

[29] P. Hosur, X.-L. Qi, D. A. Roberts, and B. Yoshida, Chaos in quantum channels, J. High Energy Phys. 02 (2016) 004.

[30] V. Alba and P. Calabrese, Quantum information dynamics in multipartite integrable systems, Europhys. Lett. **126**, 60001 (2019).

[31] R. Modak, V. Alba, and P. Calabrese, Entanglement revivals as a probe of scrambling in finite quantum systems, J. Stat. Mech.: Theory Exp. (2020) 083110.

[32] V. Balasubramanian, A. Bernamonti, N. Copland, B. Craps, and F. Galli, Thermalization of mutual and tripartite information in strongly coupled two dimensional conformal field theories, Phys. Rev. D **84**, 105017 (2011).

[33] A. Allais and E. Tonni, Holographic evolution of the mutual information, J. High Energy Phys. 01 (2012) 102.

[34] L. Nie, M. Nozaki, S. Ryu, and M. T. Tan, Signature of quantum chaos in operator entanglement in 2d CFTs, J. Stat. Mech.: Theory Exp. (2019) 093107.

[35] J. Kudler-Flam, M. Nozaki, S. Ryu, and M. T. Tan, Quantum vs. classical information: Operator negativity as a probe of scrambling, J. High Energy Phys. 01 (2020) 031.

[36] J. Kudler-Flam, Y. Kusuki, and S. Ryu, Correlation measures and the entanglement wedge cross-section after quantum quenches in two-dimensional conformal field theories, J. High Energy Phys. 04 (2020) 074.

[37] A. Zabalo, M. J. Gullans, J. H. Wilson, S. Gopalakrishnan, D. A. Huse, and J. H. Pixley, Critical properties of the measurement-induced transition in random quantum circuits, Phys. Rev. B **101**, 060301(R) (2020).

[38] A. Nahum, J. Ruhman, S. Vijay, and J. Haah, Quantum entanglement growth under random unitary dynamics, Phys. Rev. X **7**, 031016 (2017).

[39] B. Bertini and L. Piroli, Scrambling in random unitary circuits: Exact results, Phys. Rev. B **102**, 064305 (2020).

[40] V. Marić and M. Fagotti, Universality in the tripartite information after global quenches, arXiv:2209.14253.

[41] V. Marić and M. Fagotti, Universality in the tripartite information after global quenches: (generalised) quantum XY models, J. High Energ. Phys. 06 (2023) 140.

[42] F. Carollo and V. Alba, Entangled multiplets and spreading of quantum correlations in a continuously monitored tight-binding chain, Phys. Rev. B **106**, L220304 (2022).

[43] G. Parez and R. Bonsignori, Analytical results for the entanglement dynamics of disjoint blocks in the XY spin chain, J. Phys. A: Math. Theor. **55**, 505005 (2022).

[44] P. Calabrese, F. H. L. Essler, and M. Fagotti, Quantum quench in the transverse field Ising chain: I. Time evolution of order parameter correlators, J. Stat. Mech.: Theory Exp. (2012) P07016.

[45] P. Calabrese, F. H. L. Essler, and M. Fagotti, Quantum quenches in the transverse field Ising chain: II. Stationary state properties, J. Stat. Mech.: Theory Exp. (2012) P07022.

[46] P. P. Mazza, J.-M. Stéphan, E. Canovi, V. Alba, M. Brockmann, and M. Haque, Overlap distributions for quantum quenches in the anisotropic Heisenberg chain, J. Stat. Mech.: Theory Exp. (2016) 013104.

[47] K. Najafi, M. A. Rajabpour, and J. Viti, Light-cone velocities after a global quench in a noninteracting model, Phys. Rev. B **97**, 205103 (2018).

[48] B. Bertini, M. Fagotti, L. Piroli, and P. Calabrese, Entanglement evolution and generalised hydrodynamics: Noninteracting systems, J. Phys. A: Math. Theor. **51**, 39LT01 (2018).

[49] I. Peschel and V. Eisler, Reduced density matrices and entanglement entropy in free lattice models, J. Phys. A: Math. Theor. **42**, 504003 (2009).

[50] R. Wong, *Asymptotic Approximations of Integrals* (Society for Industrial and Applied Mathematics, 2001).

[51] V. Alba and F. Carollo, Spreading of correlations in markovian open quantum systems, Phys. Rev. B **103**, L020302 (2021).

[52] F. Carollo and V. Alba, Dissipative quasiparticle picture for quadratic Markovian open quantum systems, Phys. Rev. B **105**, 144305 (2022).

[53] V. Alba and F. Carollo, Hydrodynamics of quantum entropies in Ising chains with linear dissipation, J. Phys. A: Math. Theor. **55**, 074002 (2022).

[54] V. Alba and F. Carollo, Logarithmic negativity in out-of-equilibrium open free-fermion chains: An exactly solvable case, SciPost Phys. **15**, 124 (2023).

[55] S. Murciano, P. Calabrese, and V. Alba, Symmetry-resolved entanglement in fermionic systems with dissipation, arXiv:2303.12120.

[56] G. D. V. D. Vecchio, B. Doyon, and P. Ruggiero, Entanglement Rényi Entropies from Ballistic Fluctuation Theory: The free fermionic case, arXiv:2301.02326.